Journal of Manufacturing Systems 89 (2026) 197–214

Contents lists available at ScienceDirect

Journal of Manufacturing Systems

journal homepage: www.elsevier.com/locate/jmansys

Technical Paper

Unified Embodiment Description for functional evaluation of used components in circular manufacturing systems ☆

Jonas Hemmerich [a,*], Dominik Koch [b], Victor Mas [a], Nehal Afifi [a], Edwin Blum [b], Gisela Lanza [b], Sven Matthiesen [a], Patric Grauberger [a]

[a] IPEK - Institute of Product Engineering, Karlsruhe Institute of Technology (KIT), Kaiserstr. 10, Karlsruhe, 76131, Baden Wuerttemberg, Germany
[b] wbk - Institute of Production Science, Karlsruhe Institute of Technology (KIT), Kaiserstr. 12, Karlsruhe, 76131, Baden Wuerttemberg, Germany

ARTICLE INFO

Keywords:
Circular manufacturing systems
Remanufacturing
Degradation modeling
Condition monitoring
Functional evaluation

ABSTRACT

Circular manufacturing systems require functional evaluation of used components based on their physical state. Existing approaches describe this state from separate perspectives, such as design, manufacturing, and degradation, resulting in fragmented and incompatible representations. As a consequence, the physical state cannot be reliably linked to the functional behavior of the corresponding subsystem, which is a prerequisite for informed R-strategy decisions. This paper introduces the Unified Embodiment Description (UED), a state-dependent representation of mechanical components structured into two coupled layers. The first layer is a unified characteristic space, which adapts and extends as new lifecycle effects emerge. The second layer consists of functionally derived tolerance regions that link these embodiment characteristics to the functional behavior of the surrounding subsystem. A supporting UED method guides the systematic development of both layers. The UED is demonstrated in a case study on the spindle shaft of an angle grinder, in which manufacturing variations and degradation patterns such as polishing wear and scratches are quantified. These embodiment changes are embedded into the unified characteristic space and translated into functionally derived tolerance regions through experimental testing of the spindle-bearing subsystem. The results show that embodiment changes induced over the lifecycle can be consistently integrated within the unified characteristic space and that the relations between embodiment and functional behavior can be quantified to support R-strategy decisions. Overall, the UED provides a foundation for a state-dependent embodiment description and supports decision-making based on the functional evaluation of used components in circular manufacturing systems.

1. Introduction

Sustainability has become a central objective in production and product development, with the circular economy emerging as a key concept to decouple economic growth from resource consumption. Within this context, various R-strategies such as repairing, remanufacturing, and recycling enable different pathways for extending product lifecycles or recovering materials. However, these strategies involve an inherent trade-off between retaining the value embodied in used products, such as repair or remanufacturing, and enabling innovation through future product development [1,2].

To reconcile this trade-off, the concept of the circular factory has been proposed as a circular manufacturing system that combines value retention with product innovation through the reuse of components and subsystems in new product generations [3]. In the circular factory, reused products are no longer evaluated solely against their original specifications but must satisfy evolving functional requirements. This shifts the perspective on the trade-off between value retention and innovation toward the question of whether the available component remains capable of fulfilling the required functional behavior under changing conditions [4].

Existing approaches for evaluating R-strategies commonly rely on criteria such as cost, time, resource consumption, or emissions [5,6]. While these criteria are essential for economic and environmental sustainability, the system performance is typically only indirectly captured via indicators such as quality or feasibility [7]. However, ensuring that circular products fulfill functional requirements necessitates an explicit evaluation of functional behavior. The required functional behavior can be specified as part of requirements engineering, for example through the formalization using SysML [8]. The realized functional behavior, in turn, is not directly specified but emerges from the embodiment

☆ This article is part of a Special issue entitled: ‘Towards Circular Factories’ published in Journal of Manufacturing Systems.

* Corresponding author.
E-mail address: jonas.hemmerich@kit.edu (J. Hemmerich).

https://doi.org/10.1016/j.jmsy.2026.08.010
Received 30 April 2026; Received in revised form 18 July 2026; Accepted 27 August 2026
Available online 12 September 2026

of a technical system and its interaction with the environment, such as contact conditions or applied loads [9]. This embodiment comprises the geometry and material of the components [10] and can be described through characteristics that capture these properties in a structured manner [11]. Both perspectives on behavior are reflected in the Function-Behavior-Structure (FBS) framework [12], which distinguishes expected behavior and behavior derived from structure. Consequently, decision-making in the circular factory relies on bridging the two by linking the embodiment of a specific component to the corresponding functional behavior it achieves.

The decision-making can be illustrated by a used product returning to a circular manufacturing system. There, it passes through the successive stages of disassembly, inspection, reprocessing, and reassembly. At each stage, decisions must be made based on the embodiment state of the individual product instance. A component can be reused directly, reprocessed before reuse, or recycled if it can no longer be technically recovered. As a representative example, consider an angle grinder as a mass-produced power tool with high functional integration. Its bevel-gear stage consisting of gears, shafts, and bearings is to be transferred from the returned product into the current product generation. Thereby, two changes occur simultaneously. The functional requirements have evolved, for example toward reduced vibration levels and higher power output. At the same time, the embodiment of the components has deviated from its nominal state. This deviation remains within specified tolerances due to manufacturing or exceeds them due to subsequent degradation. Assessing the embodiment state and its impact on functional behavior then leads to a decision for each component. The gears may be recycled and replaced by the design of the current generation to meet the increased requirements, while the shafts are reprocessed to restore their surface quality and the bearings are reused directly as they show no relevant degradation.

This example demonstrates that, in contrast to conventional design scenarios, the embodiment of reused components does not correspond to a well-defined state. Instead, it results from the superposition of multiple influences converging in the circular factory: (1) Degradation mechanisms accumulated during prior use alter the embodiment of incoming components instance-specifically. They can shift characteristics beyond their specified tolerance limits and introduce additional characteristics that are not part of the nominal design. (2) Manufacturing processes in linear production and reprocessing cause other deviations from the intended embodiment. They act on existing characteristics and, given sufficient process capability, remain within their specified tolerances. (3) Intentional design changes in product development additionally modify the nominal embodiment to adapt to new requirements. Such intentional changes concern the design of the new product generation as well as adaptations of components from previous generations to enable their transfer. These influences interact in potentially conflicting ways, so that evaluating functional behavior requires a consistent description of heterogeneous and evolving embodiment states. Current approaches in engineering design, manufacturing, and degradation analysis address this challenge only in a fragmented manner, as they describe embodiment states from domain-specific perspectives. Design methods focus on the nominal embodiment state [10], tolerance analysis and uncertainty-based design on manufacturing-induced deviations [13,14], and condition monitoring on the temporal evolution of functional behavior caused by degradation [15]. Across these perspectives, embodiment is described either as an idealized design state, as a deviation from nominal specifications, or indirectly through behavior metrics, but not as the superimposed state of an individual used component.

As a consequence, the selection of R-strategies at the instance-specific component level lacks a systematic basis for decision-making in circular manufacturing systems. The central problem is that embodiment states, which may extend beyond specified manufacturing tolerances and involve characteristics not part of the nominal design, cannot be consistently compared across instances, product generations, and manufacturers with respect to their impact on functional behavior. This leads to the following research question: *How can the superimposed embodiment of a component be described in a way that enables systematic quantification of its impact on functional behavior for decision-making in circular manufacturing systems?*

To address the research question, this paper introduces the Unified Embodiment Description (UED) as a state-dependent representation of mechanical components based on the superposition of functionally relevant embodiment characteristics. Structured into two coupled layers, it combines a unified characteristic space that captures lifecycle-induced embodiment changes with functionally derived tolerance regions that link these characteristics to the functional behavior of the corresponding subsystem. The UED is developed by first deriving the requirements that such a description must fulfill from the role of functional behavior in the decision-making process and from the analysis of various used products from the power tool domain, then reviewing existing approaches against these requirements, and synthesizing their relevant aspects, complemented where necessary, into the proposed representation. The case study serves to demonstrate the application of the UED and to derive first insights about the representation and its supporting method.

The main contributions of this paper are as follows:

1. A UED for representing lifecycle-induced state changes of mechanical components and supporting decision-making in circular manufacturing systems through comparison of achievable functional behavior with corresponding requirements.
2. A supporting UED method that guides the systematic development by identifying and evaluating functionally relevant embodiment characteristics arising from design intent, manufacturing-induced deviations, and degradation effects.
3. An experimental case study on the spindle shaft of an angle grinder demonstrating the construction of the two UED layers under real-world conditions.

The remainder of this paper is structured as follows. Section 2 reviews existing approaches for describing embodiment and its relation to functional behavior. Section 3 presents the conceptual basis of the UED and the procedure of its supporting method. Section 4 reports the results from the experimental case study on the spindle shaft. Section 5 discusses the concept of the UED and its implications for circular manufacturing systems, while Section 6 concludes the paper and outlines directions for future research.

2. Related work

This section derives the requirements that a description of embodiment and its relation to functional behavior must fulfill to support decisions in circular manufacturing systems, and reviews existing approaches against them. Evaluating whether a used component can be reused, reprocessed, or recycled requires linking its physical state to the functional behavior of the corresponding subsystem. From this decision situation and the observed embodiment states described above, several requirements follow. The description must capture deviations from the nominal state and refer to the individual returned instance rather than a component type. Since degradation can introduce characteristics that are not part of the nominal design, the set of characteristics must be adaptive rather than fixed. The described embodiment must be related to functional behavior, and this relation must be quantified rather than remain qualitative. Where reuse decisions depend on tolerances, an admissible region within the characteristic space is required, and the underlying information must be available across the lifecycle. These requirements guide the following review and serve as the criteria for the comparison in Table 1. The review is structured along three perspectives of embodiment influences, namely design-oriented representations of nominal embodiment, manufacturing-related approaches addressing stochastic variations, and degradation-focused methods capturing time-dependent changes in condition. Approaches for managing and integrating product information over the lifecycle are considered within these perspectives, as they provide the required data infrastructure for decision-making.

2.1. Description of embodiment

In **engineering design**, embodiment constitutes the tangible realization of design decisions and provides the basis from which a component's functional behavior emerges. A widely used approach to describe the nominal embodiment is through characteristics, which capture geometric and material properties in a structured manner [11]. The description using such characteristics is guided by established standards and norms, such as the Geometrical Product Specifications (GPS) [16]. These specifications define nominal values and tolerance ranges for dimensions, form, and positional relationships in technical drawings, and allow the nominal embodiment to be fully represented in digital computer-aided design environments. The tolerance ranges bound the admissible deviation from the nominal values, but they do not represent the actual deviation of an individual manufactured or degraded component. These descriptions are therefore limited to the ideal component state and insufficient for evaluating embodiment in scenarios involving deviations caused by manufacturing or degradation, as encountered in circular manufacturing systems.

In industrial practice, **manufacturing**-induced variations are addressed through quality management and tolerance analysis. For linear manufacturing, product quality is typically ensured through structured quality assurance processes, in which components are verified against defined specifications either by sampling or 100% inspection [17]. These methods operate as verification procedures against nominal specifications and do not provide a detailed representation of the actual as-manufactured geometry. To address this, tolerancing research provides approaches for representing and analyzing geometric variations beyond nominal specifications. Within tolerancing, the GeoSpelling framework is of particular interest, as it builds directly on the GPS concept by incorporating so called skin models [18]. Skin models represent the real physical surface of a component, including both ideal and non-ideal geometric features resulting from manufacturing processes. By admitting such non-ideal features, the description is not restricted to the nominal characteristics but can be extended with additional descriptors of the observed geometry. On this basis, deviations of geometric embodiment characteristics can be derived and used for tolerance analysis, virtual assembly, and evaluation of geometric variability [19]. In addition, real components, including degradation effects, have been characterized [20]. While a skin model can represent the surface of an individual component, it is typically populated from variation observed across a set of manufactured instances, so that the individual instance is captured only partially. Tolerancing approaches such as GeoSpelling furthermore do not account for the dynamic evolution of embodiment including the adaptation of characteristics over the product lifecycle.

In circular manufacturing systems, **degradation** is a key source of embodiment variability that cannot be captured by fixed inspection assumptions, but requires adaptive evaluation strategies [21]. To evaluate the condition of returned components, vision-based sensor systems combined with image processing techniques have been widely adopted [22]. These approaches enable detection and classification of surface defects such as fatigue, wear, and cracks [23,24], as well as quantitative characterization from 2D and 3D measurement data as a basis for data-driven reprocessing decisions [25]. Recent advances in machine learning further enable the automated extraction of quantitative defect descriptors directly from image data, which operate on localized image information and generate geometric descriptors of affected embodiment regions. For example, Wu et al. [26] demonstrate the automated measurement of scratch length using segmentation-based methods. Van Maele et al. [27] describe local pitting damage on helical gears using geometric features such as position, size, and shape, while Zou et al. [28] investigate fretting wear-fatigue in press-fitted axles, quantifying degradation through characteristics such as wear depth, length, and orientation. Still, most methods focus on defect detection or classification rather than a holistic geometric description of the affected component. Even when quantitative descriptors are available, they are typically case-specific and treated as a set of local discrete observations rather than a continuous modification of the global embodiment.

Independent of the perspective, the resulting embodiment is represented and managed in digital formats and systems. Standards such as STEP [29] provide a neutral representation of product geometry, while the acquisition of used components through 3D scanning yields discretized representations such as point clouds or triangulated surface meshes. Product data management and product lifecycle management systems organize these representations across the lifecycle including end-of-life stages [30,31]. Both materialize or administer the real geometry of an individual component in full detail, but establishing a set of embodiment characteristics that can be related to functional behavior and R-strategies requires an interpretation of the acquired embodiment.

2.2. Relation between embodiment and functional behavior

The described embodiment becomes relevant for decision-making only when it is related to a corresponding functional behavior. This relation between embodiment and functional behavior has been addressed at different levels of abstraction in **engineering design**. Conceptual frameworks such as the FBS framework [12] distinguish function, behavior, and structure as core elements of product design. Relevant extensions of this framework incorporate lifecycle-related aspects, such as manufacturability [32] or Design for Upgrade and Remanufacturing guidelines [33]. A related but distinct line of work introduces the function-behavior-state modeler, which makes the physical condition of a system explicit by defining a state as a set of attributes and behavior as the sequence of state transitions caused by physical phenomena [34]. Again, this conceptual framework has been applied to lifecycle-oriented design tasks such as upgradability [35]. The state modeling acknowledges that the set of attributes describing an entity is not necessarily fixed, as the structure of a system may change over its lifetime. However, structures and states are represented qualitatively for reasoning in conceptual design and are not quantified for a specific physical component, which the authors themselves identify as a limitation for industrial relevance.

More detailed approaches analyze functional behavior through parameter-based models, which relate systematically varied design parameters to the resulting behavior [36]. Design of Experiments (DoE) provides a systematic variation of these parameters and supports the identification of significant factors and their interactions [37]. The resulting functional behavior is evaluated by testing [38], either in simulation studies relying on physics-based models such as finite element analysis [39] or in experimental settings on physical components [40]. Both are increasingly combined with data-driven methods to reduce the effort associated with testing [41]. Across these methods, the varied parameters are design variables of the nominal component, so that the relation is established for the intended design rather than for the deviated state of an individual, degraded component.

Beyond the intended design, further approaches explicitly account for the effect of **manufacturing**-induced variations on functional behavior. Solution space engineering identifies the region of design parameters within which the required performance is maintained despite tolerances and uncertainties [42]. Building on such solution spaces, margin-based approaches [43] and their formalization in the Margin Value Method [44] quantify the distance between the chosen design and the boundary of the admissible space, expressing the reserve that

Table 1
Comparison of existing approaches for describing embodiment and its relation to functional behavior. Each approach is assessed against the criteria required for instance-specific decision-making in circular manufacturing systems. No approach fulfills all of them.

Legend: ● addressed; ◐ partially addressed; ○ not addressed

Approach	Ref.	Requirements: Deviations from nominal state	Individual instances	Adaptive characteristic space	Functional evaluation based on embodiment	Quantitative functional behavior	Admissible characteristic space	Lifecycle data integration
Describing embodiment (Section 2.1)								
GPS and CAD-based description	[16]	◐	○	○	○	○	○	○
GeoSpelling and skin model shapes	[18,19]	●	◐	◐	○	○	○	○
Vision-based degradation assessment	[22,26]	●	●	◐	○	○	○	◐
STEP and 3D scan formats	[29]	●	●	○	○	○	○	○
PDM and PLM systems	[30,31]	○	◐	○	○	○	○	●
Relating embodiment to functional behavior (Section 2.2)								
Function-behavior-state modeler	[34,35]	○	○	◐	●	○	○	○
Solution space and design margins	[42,44]	◐	○	○	●	◐	●	○
Robust design	[45]	◐	○	○	●	◐	○	○
Parameter-based models and DoE	[36,37]	○	○	○	●	●	◐	○
Condition monitoring and PHM	[46,47]	◐	●	○	◐	●	◐	◐
Artificial damage testing	[48]	◐	●	○	●	●	◐	○
Digital twin	[49,50]	○	●	○	◐	○	○	●

is kept to accommodate uncertainty and to enable later change. Robust design approaches address the same relation from the opposite direction by reducing the sensitivity of functional behavior to manufacturing and operational variation [45]. These approaches share the premise of a prospective design task, in which admissible spaces, margins, and robustness are determined for a component type before manufacturing, based on an anticipated distribution of variation within a fixed set of design parameters. They therefore do not address the evaluation of an individual, already degraded component against changed requirements, where the characteristic space itself may need to be extended by newly emerging degradation features.

In contrast, **degradation** effects are primarily addressed in condition monitoring and predictive maintenance approaches, which focus on monitoring the functional behavior of components during operation [46]. Sensor-based methods analyze signals such as vibrations or displacements to detect damage and estimate remaining useful life [47]. While these approaches capture the temporal evolution of functional behavior and can continuously integrate data over the operational life, degradation is inferred from changes in measured signals, whereas the corresponding embodiment changes are not explicitly quantified. Even when inspection data are used to relate embodiment measurements to physical degradation, this mapping is often non-systematic and strongly dependent on operating conditions and observed damage patterns [28]. To enable controlled analysis of degradation effects, some studies introduce artificial damage to investigate its influence on functional behavior under defined conditions [48], thereby establishing an explicit relation between the embodiment change and the resulting functional behavior. However, the damage is synthetic rather than derived from real use, and the analysis is centered on an isolated degradation mechanism rather than on a representation that adapts to the combination of characteristics observed on an individual component.

Beyond these individual perspectives, integrating approaches bring embodiment and behavior data together across the lifecycle. The concept of the digital twin links a physical entity to a virtual representation through data acquired over its life [49]. For remanufacturing, this concept has been formalized into an information model that defines the classes and attributes required to decide on the treatment of a returned component, spanning as-designed, as-built, and current-state representations as well as predicted future states [50]. While it provides attributes for embodiment characteristics and their deviations, it does not specify which of them are functionally relevant, nor how they relate to the resulting functional behavior. The authors accordingly identify the need to translate existing knowledge and data into an integrated system, which for the embodiment of an individual, degraded component has to be derived first [50].

2.3. Positioning of the present work

The positioning of the present work with respect to existing approaches is summarized in Table 1. The comparison deliberately spans approaches of different nature, ranging from description frameworks and inspection tools to data infrastructures and evaluation methods. It assesses not their respective purpose, but whether they address the required criteria fully, partially, or not at all. Approaches for describing embodiment capture deviations from the nominal state and, in the case of vision-based methods, the state of an individual component, but they do not relate the described embodiment to functional behavior. Conceptual frameworks such as the function-behavior-state modeler evaluate behavior on the basis of the embodiment and even allow the set of attributes to change, but they remain qualitative and do not quantify the relation for a specific physical component. Parameter-based models quantify this relation for systematically varied design parameters, and solution space engineering and robust design build on such relations to derive admissible regions or margins. However, all of them operate on idealized nominal geometries and anticipated distributions of variation for a component type. Condition monitoring approaches capture the state of an individual component over time, but infer degradation from measured signals rather than describing the underlying embodiment. Artificial damage testing establishes this relation from the embodiment side, but only for isolated and synthetic defects. Digital twin approaches integrate embodiment and behavior data across the lifecycle, but provide the architecture in which such data are organized without specifying which characteristics are functionally relevant. Across all considered approaches, the set of characteristics is furthermore not adapted to newly emerging degradation features. It either remains fixed, is extended only qualitatively or in a predefined manner, or captures new features as isolated local observations without integrating them into the global embodiment. Each of the required criteria is therefore met by some of the reviewed approaches, but not within a single integrated one. No existing approach combines an adaptive, instance-specific embodiment description with a quantitative relation to functional behavior, which is the gap addressed by the UED introduced in this work.

3. Proposed approach

The fragmented representation of embodiment states and its relation to functional behavior motivates a structured approach for consistent decision-making in circular manufacturing systems. This section introduces the UED that integrates design, manufacturing, and degradation perspectives into a single characteristic-based and state-dependent

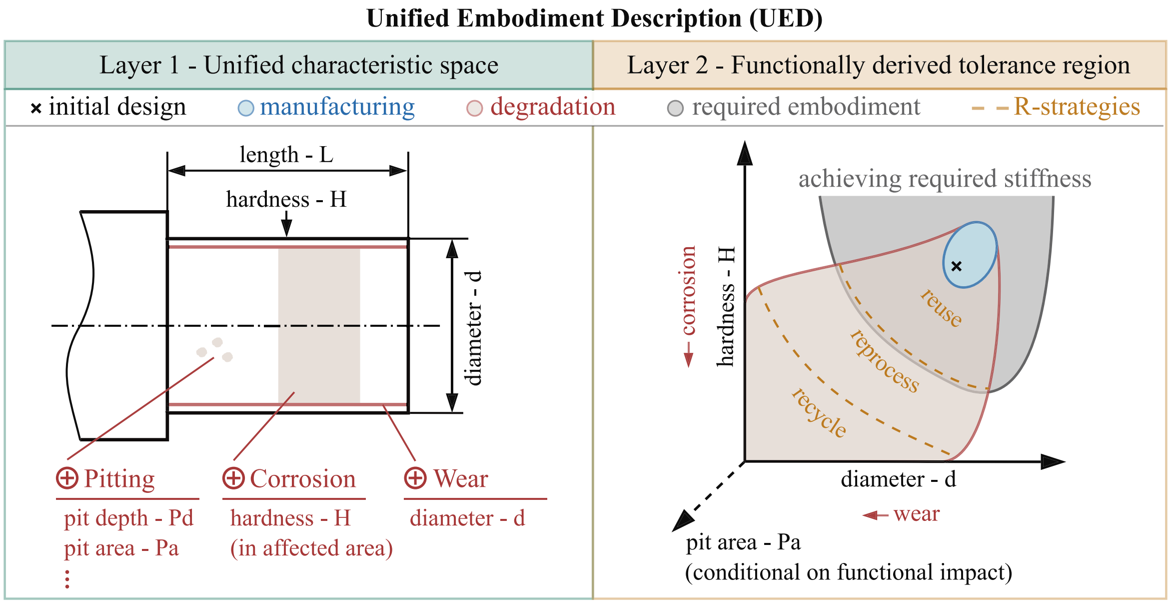

Fig. 1. Layer 1 shows nominal design characteristics (black) and degradation-induced descriptors (red). Layer 2 adds manufacturing variations (blue), required embodiment space (gray), and R-strategy boundaries (orange), arranged by increasing intervention depth. (For interpretation of the references to color in this figure legend, the reader is referred to the web version of this article.)

representation. The UED denotes the two-layered description scheme, which is constructed by the supporting UED method. The scheme defines how embodiment characteristics and functionally derived tolerance regions are structured, while the method specifies the procedure by which both layers are constructed. Applying the approach to an individual component yields its instance-specific embodiment description, which serves as the basis for R-strategy decisions. The UED is described according to established guidelines for design methods using the four elements of intended use, core, representation, and procedure [51].

3.1. Unified Embodiment Description

The **intended use** of the UED is to support decision-making for returned mechanical components in circular manufacturing systems, where the embodiment state deviates from the nominal design beyond the specified manufacturing tolerances and involves characteristics that are not part of the nominal design. It enables the assessment of whether a component can be reused, requires reprocessing, or should be recycled by linking observed embodiment states to functional requirements under evolving characteristic conditions. The acquisition, storage, and integration of the required data across the lifecycle are not part of the UED and remain a task for the surrounding information architecture, such as a product digital twin. The UED is applied during the development phase of the next product generation, prior to factory operation, by engineers with existing design knowledge of the technical system.

The **core** of the UED is based on the principle that all lifecycle-induced changes in mechanical components can be consistently captured through the definition of embodiment characteristics, provided that they manifest as measurable geometric or material characteristics. Latent effects without a measurable signature at the considered point in time, such as fatigue that has not yet led to a detectable change in the embodiment, are therefore outside the scope of the description. By using embodiment characteristics as central element, the UED enables a coherent and comparable description of component states across lifecycle stages and supports the systematic analysis of their impact on functional behavior.

On a structural level, the **representation** of the UED consists of two coupled layers, a unified characteristic space and functionally derived tolerance regions defined within this space. The two layers decouple the embodiment characteristics themselves from their corresponding tolerances. This separation is necessary because functional requirements may vary across product generations and usage conditions, while degradation can alter the relevance and interaction of embodiment characteristics over time. Fixed characteristic-specific tolerance definitions are therefore insufficient to capture evolving functional constraints. Fig. 1 illustrates the layer structure for a simplified shaft, which serves as an example throughout this section.

The first layer is the unified characteristic space, which represents the embodiment state of a component. Nominal design definitions provide the initial reference state, while degradation can shift characteristics beyond the specified tolerances and introduces additional or modified characteristics reflecting usage-dependent changes. The space is therefore not static but adapts and extends depending on the observed embodiment state. Manufacturing-induced variation, in contrast, acts on existing nominal characteristics and is represented as the baseline distribution within the specified tolerances against which degradation-induced deviations are interpreted. In the illustrated example, the nominal design defines diameter, length, and surface hardness of the shaft. Abrasive wear reduces the diameter, corrosion decreases the surface hardness at affected areas, and pitting introduces additional descriptors such as pit depth and pit area that extend the characteristic space.

The second layer defines functionally derived tolerances within this characteristic space. Tolerance limits are not defined as independent bounds of individual characteristics, but as regions that satisfy functional requirements under multivariate interaction. These regions are obtained by evaluating combinations of characteristics with respect to functional behavior, resulting in system-level constraints rather than isolated characteristic limits. In the shown example, the functional tolerance region is derived from a required stiffness and spans the two nominal characteristics of diameter and surface hardness. The region is not axis-parallel but reflects the multivariate interaction of the characteristics, as a reduction in one characteristic can be compensated by the other while still achieving the required stiffness. Degradation caused by wear and corrosion shifts the embodiment state from the manufacturing-induced baseline toward and beyond the functional boundary. If further investigation of the pit area yields an impact on the shaft stiffness, an additional dimension needs to be considered in the characteristic space.

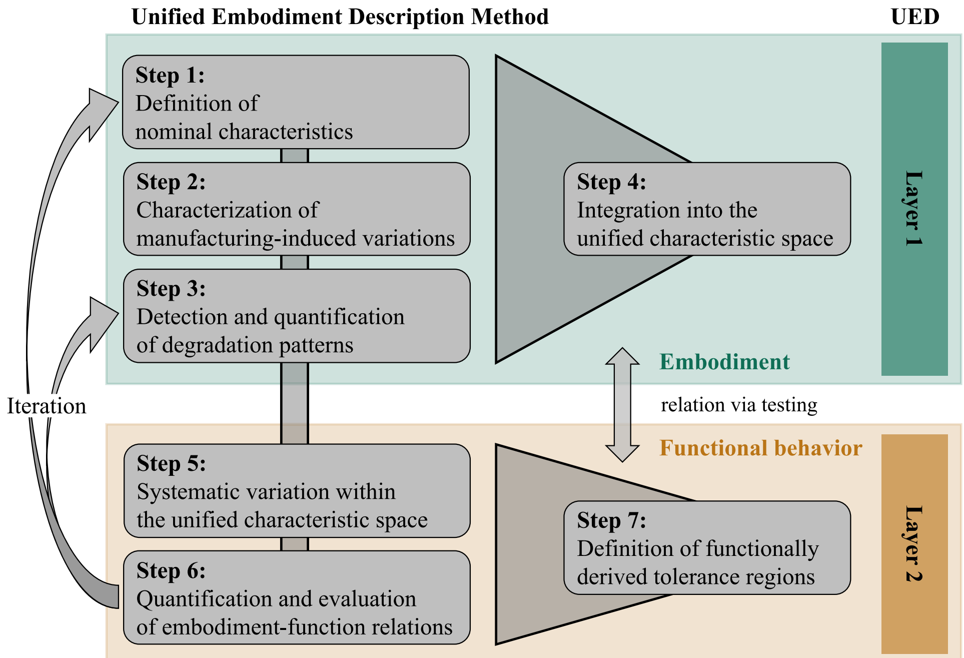

Fig. 2. Seven-step methodology for constructing the UED. Steps 1–4 establish the unified characteristic space (layer 1) by integrating design and degradation information. Steps 5–7 define the functionally derived tolerance region (layer 2) by linking embodiment characteristics to functional behavior, and can be revisited iteratively as new insights are gained.

The selection of an R-strategy for a used component follows from the position of its embodiment state relative to the functional tolerance region and from the technical reach of the available reprocessing operations. A state within the region already achieves the required stiffness and is therefore assigned to direct reuse. A state outside the region is assigned to reprocessing if the responsible characteristics can be restored into the region, for example by additive manufacturing or re-hardening, and to recycling if they cannot. The resulting R-strategy zones in Fig. 1 therefore represent the combination of functional fulfillment and technical manufacturing capabilities.

The **procedure** for constructing the two layers is based on the supporting UED method.

3.2. UED method

The UED method is illustrated in Fig. 2 and follows seven steps, of which the first four establish the unified characteristic space (layer 1) and the last three define the functionally derived tolerance regions (layer 2). First, nominal embodiment characteristics are identified based on functionally relevant GPS from the design definition. Second, manufacturing-induced variations are characterized to establish a reference distribution of as-manufactured components. Third, degradation effects are detected and quantified using appropriate descriptors. Fourth, these embodiment descriptors are integrated into the unified characteristic space that consistently represents the individual component state. Fifth, systematic variation of embodiment characteristics is performed to explore their influence on functional behavior. Sixth, the impact on functional behavior is quantified and evaluated based on testing. Seventh, functionally derived tolerance regions are established based on functional requirements. The method can be revisited iteratively as the evaluation gains new insights about functional relevance causing nominal characteristics or degradation descriptors to be excluded, adapted, or added.

3.2.1. Step 1: Definition of nominal characteristics

The first step identifies functionally relevant nominal characteristics based on GPS, which serve as the initial reference for all subsequent analyses. In circular manufacturing systems, they additionally serve as a cross-manufacturer and cross-generational reference for comparing geometrically similar components from different product instances. The step begins by identifying embodiment characteristics that describe the geometry in a measurable and unambiguous way, such as dimensions, form deviations, or surface-related properties. Extraction relies on the technical documentation from the previous design phase of the returned product, including technical drawings and associated specification data. Since each characteristic introduces an additional dimension, a subsequent reduction retains only those that are assumed to be relevant for functional behavior within the respective system context. This reduction is guided by defining relevant aspects of the functional behavior that are influenced by the component, such as vibration, noise, heat generation, sealing, or efficiency.

In addition to the nominal values, the tolerance specifications associated with each characteristic are extracted, as they define the variation that is admissible in linear production. While the identified characteristics populate the unified characteristic space, the associated nominal tolerances are not applied as constraints within it. Instead, they serve as a baseline for interpreting manufacturing-induced variation in step 2 and inform the derivation of functionally derived tolerance regions in step 7.

3.2.2. Step 2: Characterization of manufacturing-induced variations

For returned components, manufacturing-induced variations and degradation-induced changes cannot be strictly separated in the observed geometry, as both contribute to the same measured embodiment state. Consequently, degradation is treated as the primary source of state variation in circular manufacturing contexts, while manufacturing-induced deviations define the reference framework for interpreting geometric measurements. In addition, geometric specifications such as tolerances for surface- or form-related characteristics are often asymmetric or only partially constraining. As a result, measured values cannot be directly interpreted in isolation, as their position within the intended design space is not uniquely defined. A reference-based model is therefore required to enable consistent interpretation of geometric states.

Starting from the nominal characteristic space defined in step 1, real manufacturing data based on process monitoring or quality control are used to populate the characteristic space with observed variations. For each characteristic, its statistical distribution is analyzed with respect to bias within the tolerance range and overall scatter, revealing systematic tendencies such as shifts toward tolerance limits as well as stochastic process-related variation. The resulting baseline extends the nominal characteristic space with empirical information on manufacturing capability and supports the assessment of presence and severity of degradation patterns in the following step.

3.2.3. Step 3: Detection and quantification of degradation patterns

The third step detects and quantifies occurring degradation patterns in used components by first establishing a structured knowledge base. As this step relies on empirical measurements, it requires used components exhibiting representative degradation. The analysis is driven by individual patterns, while being consistently expressed through the use of embodiment characteristics.

The definition of the degradation knowledge base is guided by standards for machine elements, domain expertise, and empirical observations of returned components, which provide information on typical probability and severity. Based on the application context and operating conditions, relevant degradation patterns are selected and structured. For each pattern, the corresponding manifestation is defined in terms of observable embodiment effects, from which measurable features for detection and quantitative descriptors are derived. Degradation patterns are distinguished into continuous effects, which affect the overall embodiment such as abrasive wear, and discrete effects, which are localized in space such as pitting.

Drawing on the knowledge base, degradation patterns are detected and quantified using appropriate measurement strategies. The selection of a suitable strategy depends on the degradation manifestation, functional impact, and accessibility of the component and may include geometry-based approaches such as optical or tactile measurement, or behavior-based approaches such as vibration or friction analysis. Automated detection is particularly relevant for discrete degradation patterns requiring spatial localization and for components with limited accessibility. Measurement strategies and sensing systems for quantification depend on the required descriptor type and measurement resolution. The resulting measurements are evaluated against the reference distribution established in step 2 to assess whether observed deviations exceed expected manufacturing variability and can be attributed to degradation.

3.2.4. Step 4: Integration into the unified characteristic space

The fourth step integrates the outputs of the first three steps into a consistent and extendable embodiment description of the individual returned component. Depending on the detected degradation patterns and manufacturing-induced variations, the nominal state in the unified characteristic space is selectively adapted or extended. The integration therefore follows a qualitative activation logic, where additional descriptors are introduced only when the corresponding degradation patterns are present.

First, the descriptors of each detected degradation pattern are compared with the nominal characteristic space. Depending on their relation to the existing characteristics, three cases are distinguished. Cases 1 and 2 mainly occur for continuous degradation effects, whereas localized discrete damage often requires additional characteristics according to case 3.

- Case 1: Existing characteristics are sufficient.
  The degradation pattern can be expressed using an existing characteristic without modification
  (e.g., change in diameter due to wear).
- Case 2: Existing characteristics require adaptation.
  The characteristic remains relevant, but its description must be extended or reformulated
  (e.g., localized evaluation of hardness due to corrosion).
- Case 3: New characteristics are required.
  The degradation pattern is not represented in the nominal space and additional characteristics must be introduced (e.g., additional descriptors for pitting).

Afterwards, interactions between the characteristics are identified, as newly introduced degradation descriptors may not only have direct effects but also modify existing characteristics. For example, a scratch may be represented by its depth as a new localized characteristic, while simultaneously reducing local diameter and increasing roughness. Such dependencies are documented and, where necessary, incorporated into subsequent measurement and evaluation procedures.

The resulting description combines global characteristics with spatially referenced degradation descriptors. While global characteristics can be expressed as scalar values, the spatial localization of discrete degradation patterns benefits from a 3D representation of the component, in which position, orientation, and extent of localized features are unambiguously assigned.

3.2.5. Step 5: Systematic variation within the unified characteristic space

After establishing the qualitative embodiment description in step 4, the functional relevance of the individual characteristics is still unquantified. The fifth step therefore prepares the systematic evaluation by deriving a structured study design within the unified characteristic space. Instead of exhaustively varying all characteristics in a full-factorial manner, the approach follows a hypothesis-driven strategy in which knowledge of the preceding analysis is used to anticipate expected relations, likely interactions, and relevant variation ranges. Characteristic variation follows two complementary perspectives, controllable variation through design changes or reprocessing measures and inherent variation caused by degradation effects. Representative factor levels are selected to cover observed component states and to enable systematic exploration of the adjacent parameter space. The systematic investigation of degradation-related embodiment changes requires the introduction of artificial damage to realize the physical embodiment state of specimens for experimental testing.

By expressing degradation-induced and intended design changes within the same description, both domains can be jointly investigated regarding main effects, interactions, and potential compensation mechanisms. Finally, a reference state is defined representing a functionally compliant baseline, such as a new or nominally conforming component, against which the measured responses of the varied embodiment states are compared in the following step.

3.2.6. Step 6: Quantification and evaluation of embodiment-function relations

The sixth step generates and evaluates measurable data describing the functional behavior based on the study design of step 5. An appropriate testing environment is established, including experimental setups or simulation models capable of reproducing the defined characteristic variations while reliably capturing the metrics of the functional behavior. As this step comes at considerable effort, the definition of functional metrics and the establishment of the testing environment can often build on already present validation criteria, testing procedures, and performance targets from the original product development process. Subsequent data analysis identifies relevant dependencies, sensitivities, and potential interactions between characteristics. These relations are summarized in a suitable form, such as empirical models, response surfaces, threshold values, or ranked influence factors.

The outcome of this step is a reliable dataset linking embodiment variations to quantified functional responses. This provides an empirical basis for understanding how changes in embodiment affect system behavior without requiring a fully predictive physical model.

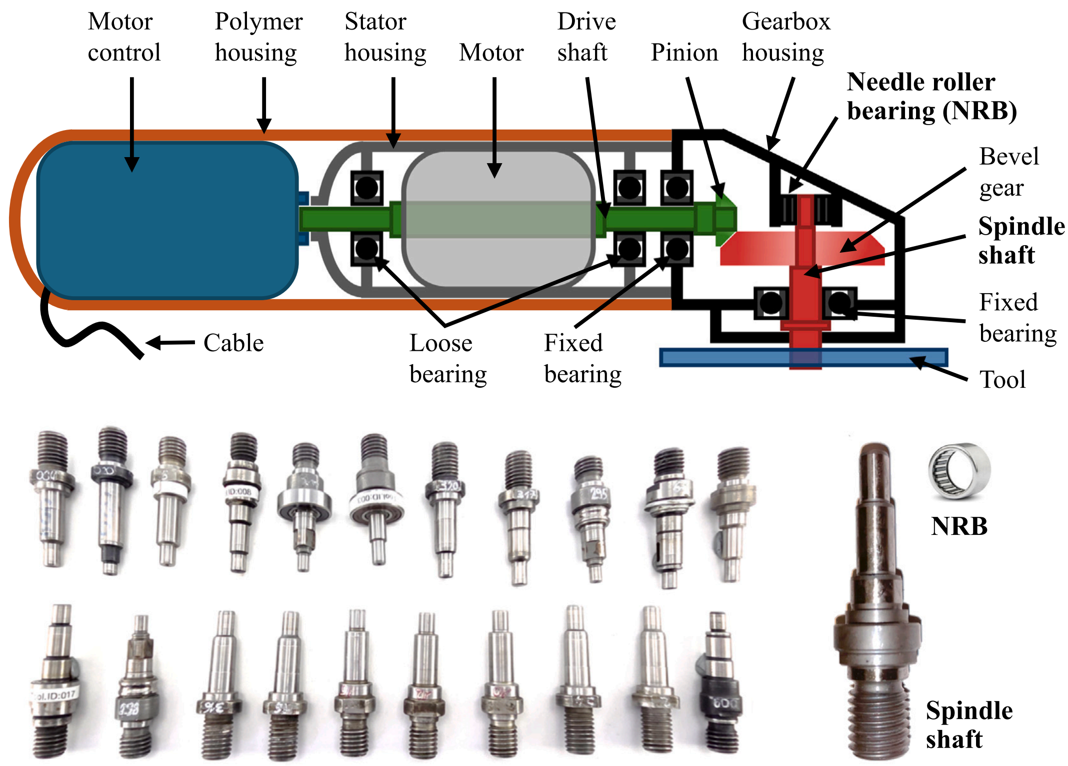

Fig. 3. Principal sketch of the *Fein CG15-125BL* angle grinder based on [52], showing the product structure with relevant components (top). The bottom view details the spindle shaft, needle roller bearing (NRB), and the full set of analyzed spindle shafts.

3.2.7. Step 7: Definition of functionally derived tolerance regions

The seventh step derives practically applicable characteristic limits from the quantified relations between embodiment variation and functional behavior. These limits form the basis for decision-making on the suitable R-strategy for a used component within a circular manufacturing system. First, the functional requirements of the investigated product variant must be specified. Based on these requirements, tolerance regions associated with sufficient functional behavior are identified and linked to the responsible embodiment characteristics, considering both individual effects and relevant interactions.

The resulting tolerance regions define the decision rule that links an observed embodiment state to a suitable R-strategy. If the observed characteristic values lie within the functional region, the component fulfills the requirements and is assigned to direct reuse. If they lie outside, the decision depends on whether the responsible characteristics can be technically restored into the region, which is feasible only if the available reprocessing capabilities, for example additive and subsequent subtractive operations, can establish the required characteristic state. If they cannot, the required functional behavior is not recoverable and the component is recycled. Embodiment states close to R-strategy boundaries may additionally warrant intensified inspection to account for measurement and prediction uncertainty. Beyond this functional decision rule, manufacturing, assembly, and economic constraints should also be considered when defining practically applicable boundaries, in accordance with multi-criteria decision models.

The resulting tolerance regions turn the embodiment description of an individual component into an operational decision on its further use. Beyond this short-term decision, the identified sensitivities and recurring degradation patterns can be transferred to future product generations, thereby supporting more robust designs for circular use.

4. Case study

The following case study demonstrates the application of the UED method in a circular manufacturing context for angle grinders, focusing on the reuse and reprocessing of mechanically degraded components. A spindle shaft is selected as a representative component to illustrate the method under real-world engineering conditions. The analysis is restricted to geometric embodiment characteristics, while material-related effects are excluded to maintain a focused and measurable application scope.

4.1. Case description

Angle grinders are portable power tools used for cutting and grinding hard materials such as steel, concrete, or stone. Fig. 3 shows a schematic representation of the technical system and the corresponding component of the case. The spindle shaft of the output stage is selected as the investigated component due to its functional relevance. It transmits the torque of the drivetrain while supporting loads originating from the gear stage and operator-induced forces. A needle roller bearing (NRB) with drawn cup and without inner ring supports the spindle shaft in the gearbox housing. Since the needles run directly on the shaft surface, the subsystem is highly sensitive to embodiment deviations.

From a circular manufacturing perspective, returned angle grinders from different generations and manufacturers often exhibit similar subsystem architectures, creating the potential for component reuse beyond the original product instance. At the same time, differences in nominal geometry between manufacturers and accumulated degradation from prior use lead to heterogeneous embodiment states. The spindle shaft therefore represents a circular decision problem in which it has to be determined whether a used component can be directly reused, requires reprocessing, or should be recycled, and to what extent nominal design interacts with degradation effects.

The case study is based on a dataset of 63 spindle shafts, including 57 used and 6 new components originating from 10 different manufacturers. To ensure a reliable evaluation, only a subset of 21 used spindle shafts from five different manufacturers (A–E), as shown in Fig. 3, was considered, as this subset provided a sufficient number of samples

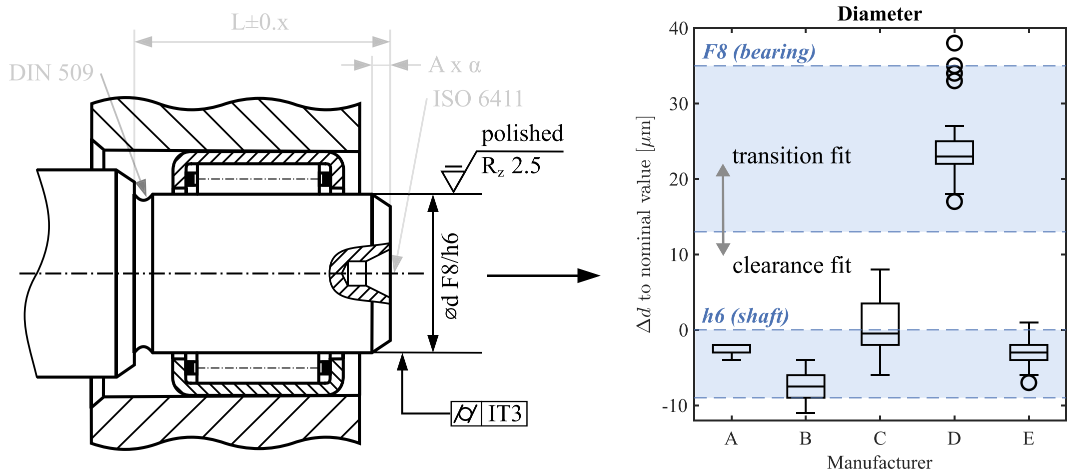

Fig. 4. Technical drawing of the spindle-bearing interface (left) and diameter measurements from five manufacturers A–E (right). Based on ISO 3245, relevant embodiment characteristics are extracted, with the measurements highlighting manufacturer-specific fit strategies.

for drawing valid conclusions. For the purpose of cross-manufacturer compatibility in the steps 1–4 and functional evaluation in the steps 5–7, the *Fein CG15-125BL* angle grinder of manufacturer A is used as the reference perspective. This angle grinder has a nominal diameter of $d = 7$ mm and uses the *SKF HK 0709* as dedicated NRB. The embodiment is analyzed using standardized metrological procedures for new shafts and adapted measurement strategies for used shafts exhibiting degradation. To evaluate the influence of embodiment deviations on functional behavior, dedicated test specimens with artificial damage and an experimental test setup are used.

4.2. Results

4.2.1. Step 1: Definition of nominal characteristics

The nominal characteristics of the spindle shaft are defined by the requirements of its functional interface. Since the shaft surface forms a contact pair with the needles of the NRB, the relevant embodiment is governed by ISO 3245 [53], which specifies the design of a NRB with drawn cup and without inner ring, as well as the corresponding bearing seats. The nominal characteristics of the spindle shaft are therefore derived from the dimensions and tolerances defined therein. An exemplary technical drawing of the spindle-bearing subsystem, in accordance with GPS conventions, is sketched on the left side of Fig. 4. The contact pair also motivates a reduction of the characteristic set, as secondary geometric features in the form of length, chamfer, center hole, and relief groove are not dominant for the investigated functional behavior. The resulting nominal characteristic space consists of the shaft diameter (inside of h6), the shaft cylindricity (inside of IT3), and the shaft surface roughness (polished and below $R_z = 2.5\,\mu$m). In addition to the shaft diameter, the tolerance of the inner diameter of the NRB is defined as F8.

In the given diameter range the two tolerances relate to the absolute values of $[-9, 0]\,\mu$m (h6) and $[13, 35]\,\mu$m (F8). The diameter is defined by a two-sided tolerance, while cylindricity and surface roughness are constrained by one-sided limits. From a functional perspective, this implies that improved cylindricity and surface roughness have negligible impact on system behavior. However, for surface roughness, reduced friction in the bearing contact may lead to slipping instead of rolling, thereby increasing vibration levels.

To investigate cross-manufacturer and cross-generational compatibility, the right side of Fig. 4 presents the nominal diameter fit strategies applied by the five different manufacturers. Diameter measurements were performed using a digital outside micrometer (Mitutoyo Digimatic) at two axial positions outside the raceway and two radial orientations offset by 90° per position, with each measurement repeated twice and averaged. Results show that only manufacturer A dimensioned the shaft exactly to the nominal h6 tolerance, while manufacturers B, C, and E deviate but stay within a clearance fit regime. Manufacturer D far exceeds the nominal h6 tolerance, resulting in a transition fit with respect to the F8 tolerance zone of the NRB, and shows significant variation between individual product generations, which suggests that identical components are rarely reused. This variation in nominal tolerances between manufacturers highlights the importance of evaluating cross-manufacturer compatibility. It therefore has to be assessed whether components from other manufacturers still fulfill the functional requirements for the specific product variant of manufacturer A.

4.2.2. Step 2: Characterization of manufacturing-induced variations

Based on the nominal characteristic space, manufacturing-induced variations are characterized using measurements from new spindle shafts. In this case study, the measurements are carried out manually, due to missing production data. Six new spindle shafts from manufacturer A are analyzed, as they provide a consistent dataset for the as-manufactured state. The measured offsets of the shaft diameter relative to the nominal value are shown on the left side of Fig. 5. Diameter measurements were performed using the same digital micrometer and measurement scheme as in step 1. All components lie within the specified h6 tolerance zone. A slight systematic offset toward the upper tolerance limit is observed, with a mean offset of $\Delta d = -2.54\,\mu$m and a maximum offset of $\Delta d = -3.62\,\mu$m. The observed standard deviation is $sd = 0.79\,\mu$m.

A representative roundness measurement used to assess cylindricity is shown in the center of Fig. 5, obtained with an Alicona μCMM. For the given nominal diameter, IT3 corresponds to a tolerance of $2.5\,\mu$m. All measurements remain within this range, indicating no systematic manufacturing-induced variation in this characteristic.

The right side of Fig. 5 shows the measured line roughness R_z of the six spindle shafts. Measurements were acquired with a Keyence VHX-6000 digital microscope at 800× magnification, measured at four radial positions offset by 90° at the axial midpoint of the shaft. At each position, a 5 mm evaluation profile was extracted along the shaft axis with a cut-off wavelength of $\lambda_c = 0.8$ mm in accordance with ISO 4288. The mean roughness is $R_z = 2.2\,\mu$m with a standard deviation of $sd = 0.171\,\mu$m. Although all values are below the specified maximum of $R_z = 2.5\,\mu$m, the distribution lies close to the tolerance limit. For one component, a local roughness value of $R_z = 5.04\,\mu$m is observed at a specific circumferential position, which post-analysis attributes to a localized surface defect. This highlights that spatial orientation is not explicitly encoded in the nominal characteristic space, which becomes relevant for the description of degradation in step 3.

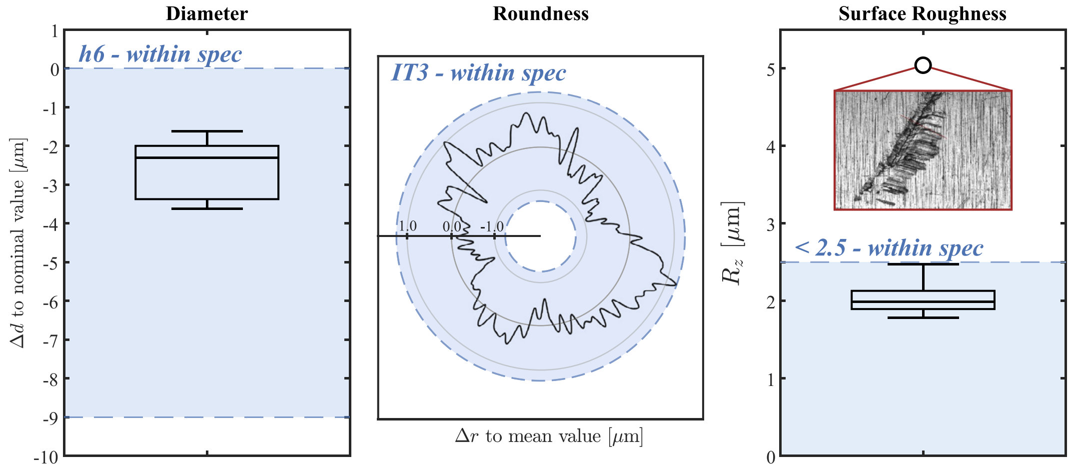

Fig. 5. Baseline measurements of diameter (left), roundness (middle), and roughness (right) from manufacturer A. Results shown as box plots against respective specification limits and as a polar profile for roundness. Characteristics are within tolerance for diameter and roundness, with a single outlier in roughness corresponding to localized surface defects.

4.2.3. Step 3: Detection and quantification of degradation patterns

The degradation knowledge base is established by combining literature-based failure classifications with empirical observations from used spindle shafts. In particular, bearing-related degradation modes according to ISO 15243 [54] are used as a structural reference, since the spindle shaft operates as the inner ring of the NRB. Combined with the screening of the 21 used spindle shafts, representative degradation patterns are selected for detailed analysis. The screening also revealed that several shafts exhibited multiple degradation patterns simultaneously, in some cases overlapping in the same region of the raceway. The resulting knowledge base links observed degradation patterns to their embodiment manifestation and corresponding geometric descriptors, as summarized in Fig. 6.

Polishing wear manifests as a reduction in surface roughness due to repeated contact between rollers and raceway and is quantified using local roughness measurements. Plastic deformation is caused by high contact stresses at the roller edges and leads to a reduction in local diameter, represented through axial diameter measurements in comparison to the nominal geometry. Scratches are local abrasive damage caused by hard particles and are represented through their spatial location and geometric descriptors such as angle, depth, width, and length. Polishing wear and plastic deformation are therefore continuous degradation patterns, whereas scratches are discrete and require localization on the component. The empirical analysis also revealed cases of fretting corrosion and pitting, which are omitted here due to scarce appearance. For the initial degradation identification, a visual pre-screening was used to localize relevant degradation features in the dataset. Since the focus of this case study is on the embodiment-based representation rather than automated inspection strategies, the detection process is not further formalized in this work.

Polishing wear is quantified with an Alicona μCMM using the same evaluation profile and cut-off wavelength as in step 2, but applied within the identified contact zone. Fig. 7 shows the results in comparison with a new spindle shaft. The worn spindle exhibits a lower mean roughness depth within the bearing contact zone, with R_z = 1.2 μm compared to R_z = 2.1 μm for the new spindle, corresponding to a reduction of approximately 43 %. This confirms that the visually identified region corresponds to a measurable modification of surface topography, consistent with the smoothing effect typically caused by polishing wear.

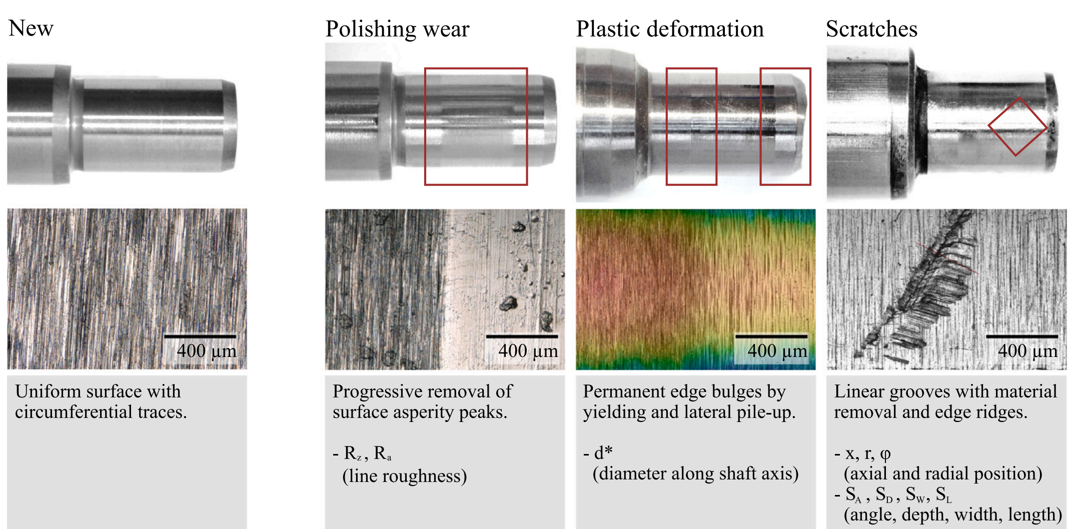

Fig. 6. Observed degradation patterns of the spindle shafts. Macroscopic view (top) where boxes mark the degradation, microscopic detail (middle) with qualitative description and measurable parameters (bottom). The new shaft serves as reference baseline. Patterns can occur individually or in combination on a single specimen. (For interpretation of the references to color in this figure legend, the reader is referred to the web version of this article.)

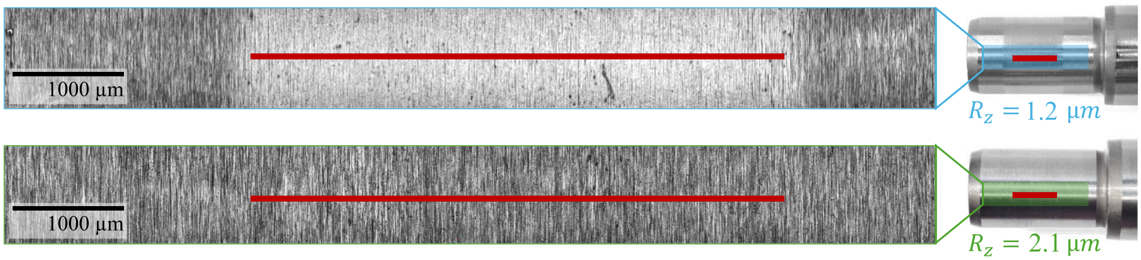

Fig. 7. Surface roughness characterization of raceway acquired with an Alicona µCMM at 20× magnification. The horizontal line indicates the 5 mm evaluation profile. Top: Used spindle with reduced surface roughness (R_z = 1.2µm). Bottom: New spindle in as-manufactured condition (R_z = 2.1µm). (For interpretation of the references to color in this figure legend, the reader is referred to the web version of this article.)

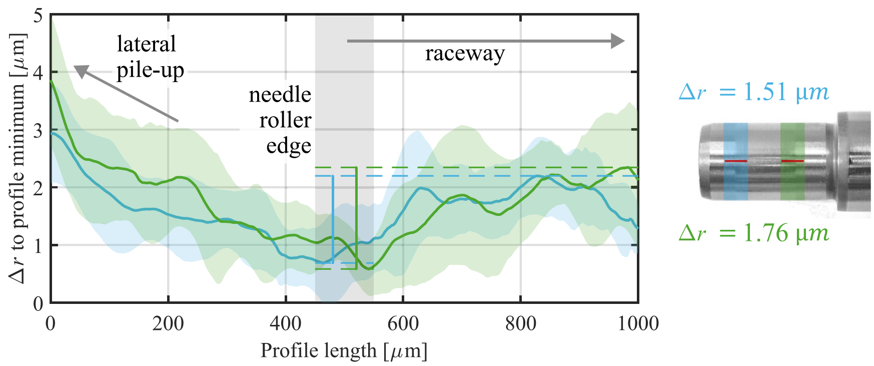

Fig. 8. Surface profile along the spindle shaft axis at the contact edge. The transition toward the bevel gear (green) shows a more pronounced radial reduction of Δr = 1.76 µm, than the shaft-end side (blue) with Δr = 1.51 µm. Both profiles rise beyond the contact edge, indicating lateral pile-up of displaced material. (For interpretation of the references to color in this figure legend, the reader is referred to the web version of this article.)

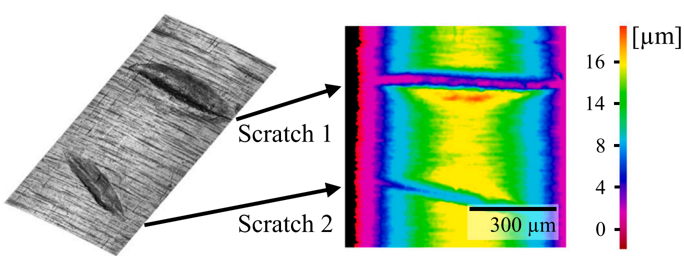

	Scratch 1	Scratch 2
Angle - S_A	89.4°	79.3°
Length - S_L	596 µm	521 µm
Width - S_W	71 µm	62 µm
Depth - S_D	12.04 µm	7.12 µm

Fig. 9. Exemplary quantification of a surface scratch using optical topography data. A perpendicular profile determines scratch width and depth via three characteristic points, while the visible extent in the image is measured along the scratch direction to determine its length.

Plastic deformation is evaluated through 3D topography measurements using a Keyence VHX-6000 digital microscope at 600× magnification, from which surface profiles are extracted. The analysis focuses on the transition regions between the bearing raceway and the nominal shaft surface, where contact-induced material flow is expected to occur. For each transition region, four profiles distributed along the circumference are recorded, with two measurement lines per angular position. The resulting radius deviations are aggregated and summarized in Fig. 8. Both transition regions exhibit a local radius reduction at the needle roller edge. Δr = 1.51 µm on the shaft-end side and Δr = 1.76 µm on the bevel-gear side. This corresponds to a mean local diameter reduction of approximately $\Delta d \approx 3.3$ µm. Beyond the contact zone, both profiles rise again toward the shaft ends, consistent with a lateral material pile-up displaced from the raceway during operation. These deviations remain within a comparable order of magnitude as the manufacturing-induced variability of the diameter established in step 2 (sd = 0.79 µm). Plastic deformation is therefore represented by adapting the existing diameter characteristic to a localized evaluation, but does not indicate a pronounced degradation effect for the analyzed sample set.

Scratches are quantified by local geometric descriptors derived from high-resolution topography measurements performed with the Alicona µCMM. For each scratch, characteristic points along and across the scratch are manually selected in the acquired point cloud, from which length and width are calculated as Euclidean distances between opposing boundary points. The depth is evaluated as the height difference between the local surface level and the minimum profile point within the groove, based on a roughness profile extracted perpendicular to the scratch orientation using a cut-off wavelength of λ_c = 0.8 mm. The orientation is defined as the angle between the principal axis of the scratch and the shaft axis, using the surface machining marks as reference. Two scratches are analyzed on the same shaft, with their geometric descriptors summarized in Fig. 9. They exhibit lengths S_L of 596 µm and 521 µm, widths S_W of 71 µm and 62 µm, depths S_D of 12.04 µm and 7.12 µm, and orientations S_A of 89.4° and 79.3° relative to the shaft axis.

4.2.4. Step 4: Integration into the unified characteristic space

The nominal characteristics diameter, cylindricity, and surface roughness are mapped to the corresponding degradation manifestations and summarized in Fig. 10. Polishing wear is assigned to case 1, as it can be directly represented by the existing surface roughness characteristic

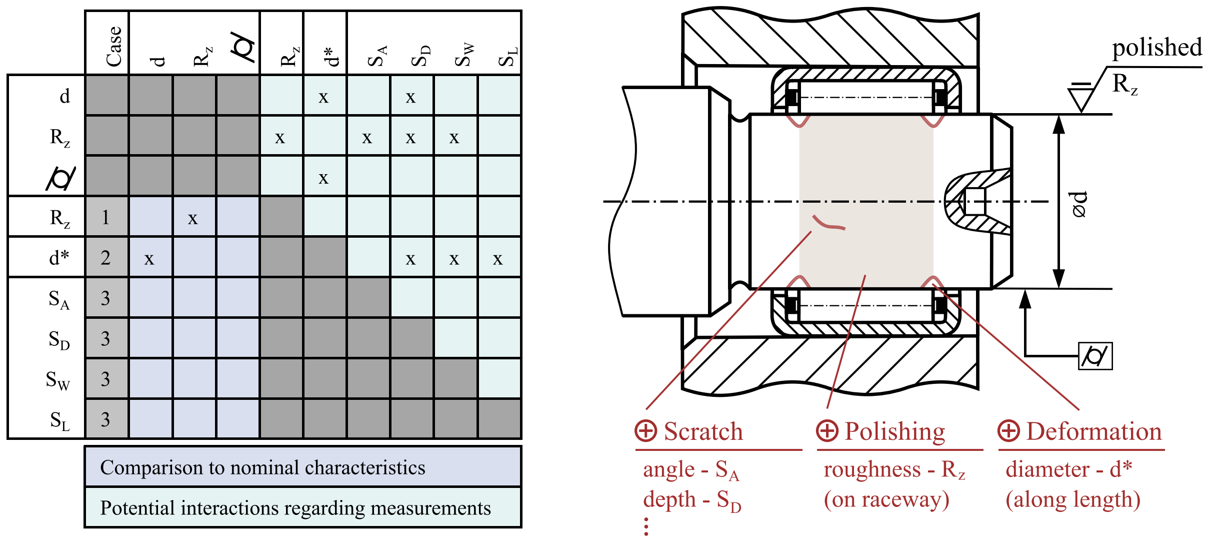

Fig. 10. Integration of embodiment characteristics including comparison and potential interactions with measurements (left). Unified characteristic space (right), including the nominal characteristic space and the degradation patterns polishing wear, plastic deformation and scratches.

without modification. Plastic deformation is assigned to case 2, since the diameter is already part of the nominal characteristic space but must be extended from a discrete measurement to a continuous profile along the shaft axis to capture local reductions. Scratches are assigned to case 3, as their occurrence introduces new, spatially localized characteristics that are not part of the original design specification. The description is reduced to orientation, length, width and depth, as a full spatially resolved representation of individual scratch positions would lead to a prohibitively high complexity for the manual case study.

In a second step, interactions between characteristics and measurement procedures are identified. A key interaction is observed between surface roughness in the nominal characteristic space and polishing wear, requiring roughness measurements to be consistently performed within the functional raceway region, where degradation is relevant. Plastic deformation introduces a continuous variation of diameter along the shaft axis, requiring multiple measurements along the raceway, particularly at the contact edges. This aligns with the measurement principle used for roundness evaluation. Scratches affect multiple measurement outcomes depending on their orientation. While diameter measurements are taken circumferentially, surface roughness is evaluated along the axial direction. Consequently, the influence of scratches on measured characteristics depends on their spatial alignment relative to the measurement direction. The resulting unified characteristic space, including all relevant characteristics and degradation-induced extensions, is shown on the right side of Fig. 10. Deviations in geometry by scratches, polishing, and deformation are highlighted in the technical drawing with red annotations, and the corresponding embodiment characteristics are listed below the associated degradation patterns. Since each inspection yields instance-specific degradation patterns and severity, the unified characteristic space adapts dynamically as further information about the embodiment is acquired. To fully exploit the UED, a spatial representation of the embodiment, for example in a 3D point cloud, can support the localization of discrete scratches and thereby improve the spatial traceability of inspection results.

4.2.5. Step 5: Systematic variation within the unified characteristic space

The parameter variation follows a staged experimental design with three phases, summarized in Table 2. In phase 1, diameter and surface roughness are varied using a full-factorial design with three levels each and one specimen per combination, resulting in 9 shafts with two measurement replications each. The shaft at diameter level 0 and roughness level 0 without scratches serves as the reference state, as its configuration corresponds to a new component. In line with the hypothesis-driven strategy of the method, the design was adapted during execution based on intermediate results from phases 1 and 2, which motivated a focused continuation in the respective subsequent phases.

An increased **diameter** enlarges the contact area between shaft and needles while reducing fit clearance, thereby affecting Hertzian contact conditions, which is expected to increase subsystem stiffness and influence vibration behavior. The factor levels are derived from nominal design specifications and manufacturing constraints. Level 0 corresponds to the nominal h6 tolerance but is tightened to IT5 for clearer differentiation between factor levels. Level +1 represents an increased diameter as observed in transition fits (manufacturer D), while level −1 reflects a reduced diameter achievable through subtractive reprocessing.

Surface roughness influences frictional conditions at the contact interface and thereby the rolling behavior of the needles. Increased roughness may lead to more localized contact and higher vibration levels, while reduced roughness may promote slip, whereas no significant effect on stiffness is assumed. The factor range combines nominal design specifications, manufacturing-induced variation, and degradation effects, with level −1 corresponding to polishing wear, level 0 to the nominal design, and level +1 to increased roughness due to wear-related surface damage. Since phase 1 revealed no significant effect of surface roughness within the investigated range, the subsequent phases were restricted to the nominal roughness level 0 to reduce experimental effort.

In phases 2 and 3, a **scratch** is introduced as a discrete degradation to capture localized disturbances expected to influence vibration behavior. The scratch location is fixed at the center of the raceway, and length and width are kept constant, while angle and depth are varied to represent characteristic extremes observed in degraded components. Phase 2 addresses scratch angle as a hard-to-change factor using a split-plot design. The three shafts from phase 1 at the nominal roughness level are reused and complemented by three additional, nominally identical shafts, yielding two shafts per diameter level with four measurement replications for each shaft. Within each diameter level, one shaft is assigned to each angle ($S_A = 0°$ and $S_A = 90°$), so that the angle is varied between subjects while all other characteristics remain fixed at a scratch depth of $S_D = 10\,\mu m$. Since phase 2 did not resolve a distinction between axial and radial scratches at this depth, phase 3 varies the scratch depth within the configurations of phase 2 to capture the effect of defect severity under identical geometric and orientational conditions. Each axial scratch is measured at an additional depth level of $S_D = 20\,\mu m$, providing a repeated-measures structure.

Table 2
Study design for functional evaluation. Phase 1 (full factorial) varies the shaft diameter d and the surface roughness R_z. Phase 2 (between shaft) and phase 3 (within shaft) vary the scratch angle S_A and scratch depth S_D.

	Phase 1: full factorial				Phase 2: between shaft	Phase 3: within shaft
Shaft ID	Level	d in mm	Level	R_z in µm	S_A in °	S_D in µm
1	−1	7e5	−1	1.50 ± 0.15	–	–
2.1	−1	7e5	0	2.50 ± 0.15	0	0/10/20
2.2	−1	7e5	0	2.50 ± 0.15	90	0/10
3	−1	7e5	+1	3.50 ± 0.15	–	–
4	0	7h5	−1	1.50 ± 0.15	–	–
5.1	0	7h5	0	2.50 ± 0.15	0	0/10/20
5.2	0	7h5	0	2.50 ± 0.15	90	0/10
6	0	7h5	+1	3.50 ± 0.15	–	–
7	+1	7s5	−1	1.50 ± 0.15	–	–
8.1	+1	7s5	0	2.50 ± 0.15	0	0/10/20
8.2	+1	7s5	0	2.50 ± 0.15	90	0/10
9	+1	7s5	+1	3.50 ± 0.15	–	–

4.2.6. Step 6: Quantification and evaluation of embodiment-function relations

To investigate the effects of the characteristic variations, empirical testing is required, as no sufficiently detailed simulation model is available and domain-specific knowledge on angle grinder spindle shafts is limited in the literature. Test specimens are therefore generated via controlled parameter variation and measured on a dedicated experimental test bench. The aim is to identify quantitative relations between embodiment characteristics and functional behavior rather than to provide a comprehensive statistical analysis, so that the number of repetitions per configuration is deliberately limited and the focus lies on comparative trends across factor levels.

The test bench is shown in Fig. 11 and also described in [55]. The original drivetrain of the angle grinder serves as power input, while a load motor and linear actuators emulate operational torque and forces. Most original components are retained to preserve realistic system behavior, while the gearbox housing is modified to enable fast exchange of the spindle shaft subsystem, comprising the spindle shaft, bearing, and bevel gear stage. This subsystem-level exchange is necessary because press fits and wear-related constraints prevent isolated shaft replacement. To ensure reproducibility across repeated assembly cycles, bearing lubrication is omitted.

The load profile represents a steady cutting operation with a load motor torque of 1.5 Nm, a horizontal actuator displacement of 200 µm, a vertical actuator displacement held at 0 µm, and an actively controlled average drive speed of 6400 min^{-1}. All signals are sampled at 18 kHz, with torque and rotational speed captured by a combined measurement shaft (HBK T210). Stiffness is derived from the reaction force at the actuator measured by a strain-gauge load cell (Burster 8435-6001), complemented by bevel gear displacement in two orthogonal directions (Keyence LK-H052 and LK-H152) as an indirect indicator of shaft deflection. Vibration emissions are captured by two accelerometers (PCB 356B21) mounted on the front and top faces of the gearbox housing, with phase 1 using the vertical component of the top-mounted sensor and phases 2 and 3 the axial component of the front-mounted sensor. Acceleration signals are evaluated as the root-mean-square (RMS) within defined frequency bands of the power spectral density (PSD), providing a scalar measure of vibration intensity per band. Broadband vibration is assessed in the gear-mesh frequency (GMF) band, while bearing-related effects are evaluated on the envelope of the acceleration signal around two characteristic kinematic frequencies of the NRB. The inner-race rotational frequency indicates eccentric loading of the shaft and the inner-race point-defect frequency indicates localized damage on the shaft surface. Results for the three phases are summarized in Fig. 12, where error bars indicate the range across repeated measurements.

Phase 1 – Diameter and roughness. The first phase investigates the influence of shaft diameter and surface roughness in the absence of scratches. The horizontal force exhibits a clear dependency on shaft diameter, with three distinct plateaus corresponding to the three diameter levels and indicating a systematic increase in subsystem stiffness with diameter. The diameter accounts for the dominant share of the variation between configurations ($\eta_D^2 = 0.94$) and its main effect

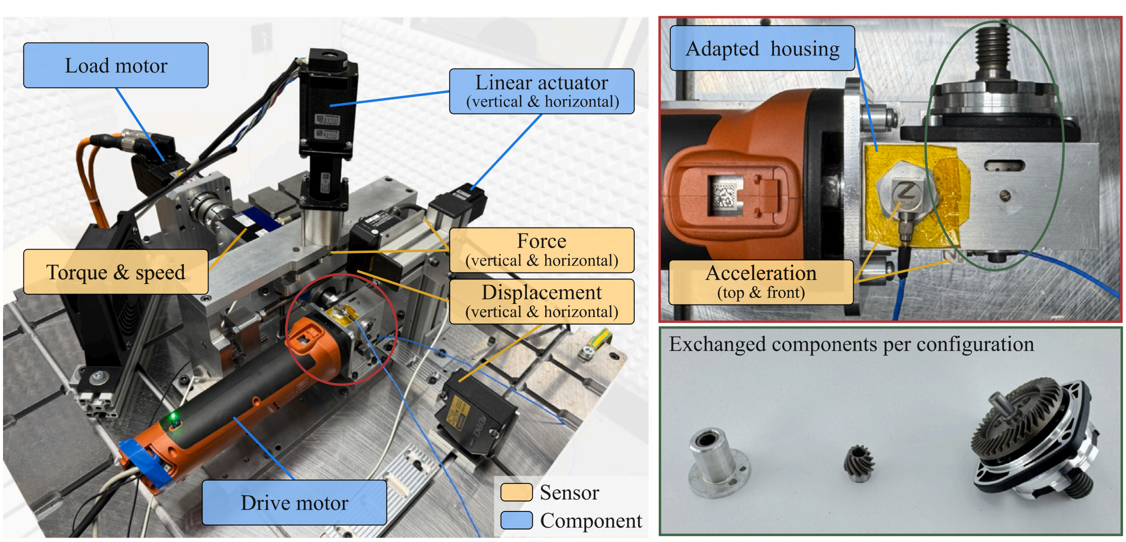

Fig. 11. Test bench for investigating the influence of the spindle shaft on stiffness and vibration. Instrumented drive train loaded with torque and forces (left), adapted gearbox housing integrating original angle grinder components (top), and exchanged shaft-bearing subsystem (bottom).

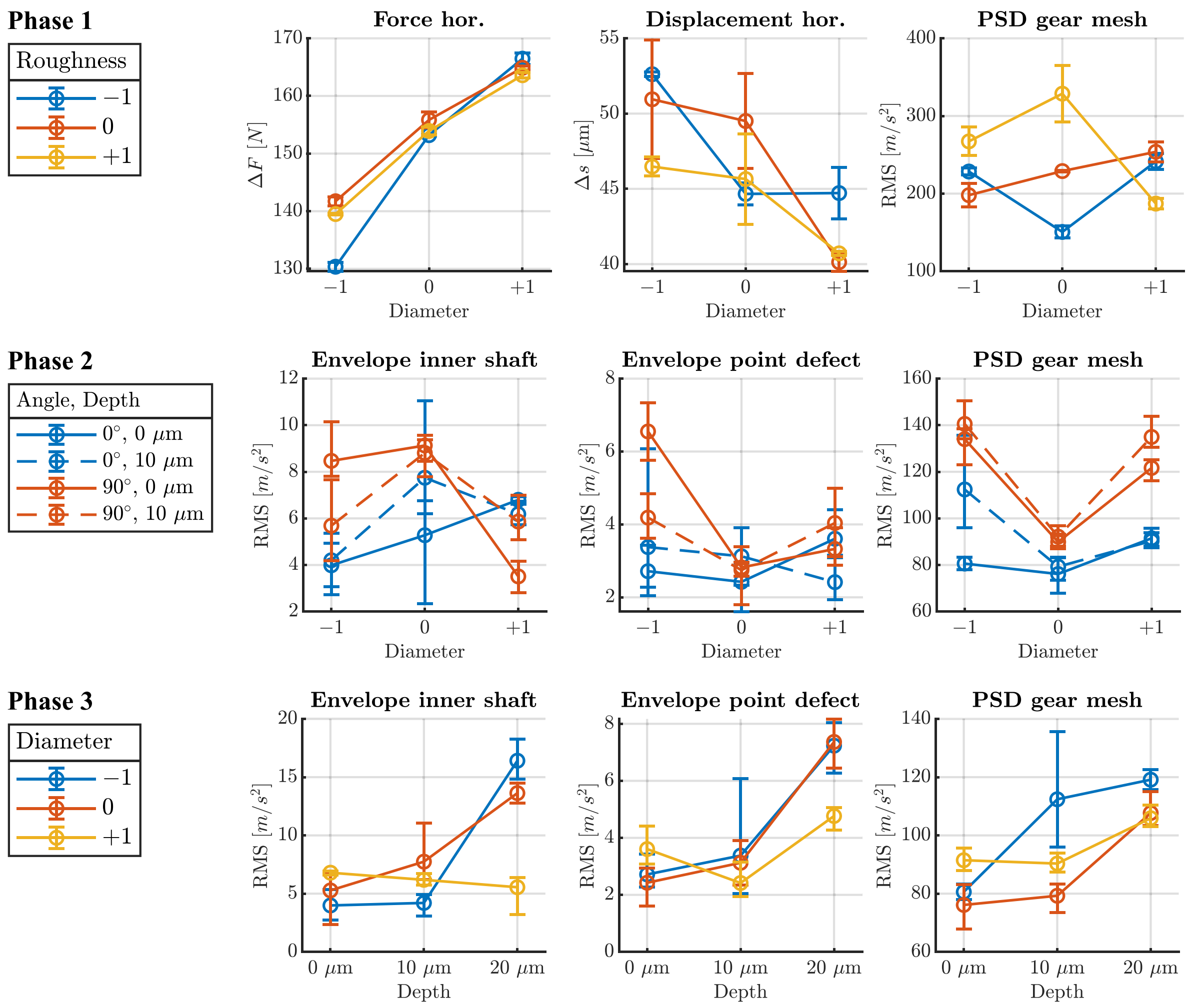

Fig. 12. Functional evaluation of shaft characteristics on subsystem stiffness and vibration across three phases. Phase 1 (top) evaluates horizontal force, axial bevel-gear displacement, and GMF-band RMS against shaft diameter and roughness. Phase 2 (center) and Phase 3 (bottom) assess envelope-based defect metrics and GMF-band RMS for scratch angle and depth in combination with shaft diameter. Error bars indicate the range across repeated measurements.

exceeds the measurement scatter by a factor of about 22, with a linear model in the diameter explaining the force almost completely ($R^2 = 0.92$). The axial displacement of the bevel gear confirms this trend as displacement decreases at higher stiffness, again well separated across diameter levels. In contrast, variations in surface roughness produce only minor differences that remain within the scatter of repeated measurements ($\eta_R^2 = 0.02$, effect of the order of the measurement scatter). The broadband vibration metric in the GMF band shows no systematic trend with respect to either diameter or roughness, and a corresponding model explains little of the observed variation ($R^2_{\mathrm{adj}} = 0.13$). Phase 1 therefore establishes diameter as the dominant driver of subsystem stiffness, while neither diameter nor roughness produces a resolvable effect on vibration within the investigated range. This negative result on the vibration side confirms that the broadband vibration signal is not systematically affected by the global characteristics and can therefore serve as a baseline for localized defects.

Phase 2 – Scratch angle. The second phase introduces a shallow scratch of approximately $S_D = 10\,\mu\mathrm{m}$ depth and varies its orientation between axial ($S_A = 0°$) and radial ($S_A = 90°$). The intent is to probe whether scratch orientation can be discriminated through the vibration response and whether the bearing-specific envelope metrics provide a more sensitive indicator than the broadband GMF-band RMS. Across all three vibration metrics and both orientations, the change induced by the scratch remains below the measurement scatter, with signal-to-noise ratios between 0.0 and 0.8 and a variance contribution of the scratch of at most $\eta^2 = 0.22$. No systematic separation between scratch orientations can be resolved. Notably, the reference measurements (solid line) taken before scratching already differ between configurations that should be nominally identical, so that a large share of the variation is attributable to differences between nominally identical shafts rather than to the scratch. In contrast, the post-scratch measurements (dashed line) remain close to their respective references. This pattern indicates that the variability is not driven by random measurement noise of the test bench, but rather by systematic effects associated with assembly and the remaining components of the subsystem. At this scratch depth, the defect-induced excitation is therefore of the same order as the global system variability, and a reliable distinction between axial and radial scratches is not yet possible.

Phase 3 – Scratch depth. Building on the findings of phase 2, the third phase isolates the effect of scratch depth by restricting the analysis to axial scratches and extending the depth range up to $S_D = 20\,\mu\mathrm{m}$. With increasing scratch depth, all three vibration metrics show a consistent upward trend, with the scratch depth accounting for the dominant share of the variation between configurations (η_S^2 between 0.51 and 0.82) and its effect exceeding the measurement scatter by a factor of about 2.1 to 2.5. The effect is most pronounced for the envelope-based metrics, where the response at the deepest scratch level clearly exceeds both the reference and the shallow-scratch level. The broadband GMF-band RMS shows a comparable, although less sharply separated, increase with scratch depth. The progression across the three depth levels is markedly non-linear. A difference between the reference state and the $S_D = 10\,\mu\text{m}$ level remains within the measurement scatter, whereas the step to $S_D = 20\,\mu\text{m}$ produces a substantial rise across all metrics. Because of this piecewise behavior, a linear model in the scratch depth captures the relation poorly, in contrast to the linear diameter–force relation established in phase 1. A categorical model that assigns a separate level to each scratch depth instead reflects the piecewise progression and explains a substantial part of the measured variation (R^2 between 0.47 and 0.71 across the vibration metrics). This indicates the existence of a detection threshold below which axial scratches cannot be reliably resolved by the considered vibration features, and above which the defect emerges clearly from the system-level variability. An interaction with the variation in shaft diameter could not be detected.

4.2.7. Step 7: Definition of functionally derived tolerance regions

Building on the quantified relations, functionally derived tolerance regions are defined for the used shafts, instantiating the decision logic for the spindle-bearing subsystem. These regions link the observed embodiment state to the R-strategies of direct reuse, reprocessing, and recycling. Their derivation rests on a set of assumptions. Diameter is treated as the dominant driver of stiffness and axial scratches as the dominant driver of vibration. Radial scratch orientation is neglected as no clear effect on vibration metrics could be shown within the given scratch depths. Since roughness does not exhibit a detectable effect on functional behavior within the examined parameter space, it is not considered as a criterion for evaluation.

For the diameter, the functional requirement is defined such that a shaft must not exhibit lower stiffness than the original component. This translates into a threshold at the lower boundary of the h5 tolerance band, corresponding to a diameter of $d = 6.994\,\text{mm}$. A shaft below this bound does not satisfy the stiffness requirement, but can be assigned to reprocessing if the missing material is re-established by additive manufacturing. This is only admissible as long as the deviation is confined to the surface layer of approximately $100\,\mu\text{m}$, since a deeper material deposition would introduce excessive heat into the component during reprocessing. Otherwise, the shaft can no longer be reconditioned and is assigned to recycling. From a purely functional perspective, no upper bound on the diameter exists, as higher stiffness is not detrimental. However, an assembly-related upper bound results from the assembly fit with the NRB, and an increasing diameter is also expected to affect long-term reliability, which remains subject to future investigation.

With respect to surface damage, the experimental results suggest a threshold-type behavior for axial scratches. Shallow scratches up to approximately $S_D = 10\,\mu\text{m}$ remain within the system-level variability and cannot be reliably distinguished from the undamaged reference, while deeper scratches in the order of $S_D = 20\,\mu\text{m}$ produce a clear and consistent increase across all vibration metrics. A maximum admissible scratch depth for direct reuse can therefore be defined around $S_D = 10\,\mu\text{m}$. Whether shafts exceeding this admissible depth can be returned into the tolerance region by subtractive and subsequent additive reprocessing, or whether the damage is too severe and the shaft must be recycled, depends on the transition between reprocessing and recycling. The precise location of this transition, in particular for a single deep scratch, is not yet quantified within the present data and remains subject to future investigation.

Overall, this instantiates the functionally derived tolerance region of Fig. 1 for the spindle shaft. Each shaft is assigned to direct reuse, reprocessing, or recycling depending on whether its embodiment state in the form of diameter and scratch depth lies within the functional region, can be shifted into it, or lies beyond the reach of the available reprocessing operations.

5. Discussion

Through the proposed approach and the subsequent case study, the research question *How can the superimposed embodiment of a component be described in a way that enables systematic quantification of its impact on functional behavior for decision-making in circular manufacturing systems?* can be answered as follows:

The UED is established as a basis for decision-making in circular manufacturing systems by systematically combining embodiment description approaches from design, manufacturing, and degradation. It is structured into two coupled layers that capture and relate lifecycle-induced effects and is constructed through a supporting UED method. On this basis, the functionally derived tolerance regions turn the assignment of R-strategies into an explicit and reproducible decision rule rather than a qualitative judgment, as demonstrated for the spindle shaft in the case study.

5.1. The UED and its supporting UED method

As a representation, the UED enables a structured description of the individually degraded embodiment of a component. Its first layer, the unified characteristic space, is not fixed in advance but adapted and extended according to the occurring manifestation of degradation. Its second layer relates these characteristics to functional behavior, so that the admissible values of a characteristic follow from the functional requirements rather than from the nominal specification of the component type. The construction of the UED is operationalized by the supporting UED method, which derives the corresponding tolerance regions for decision-making in circular manufacturing systems, such as reuse, reprocessing, or recycling of components.

Applying the UED to the spindle shaft case study reveals properties of the representation and its supporting method that only become apparent in a real application. A first strength concerns the adaptivity of the description, as degradation can alter the structure of the embodiment description itself. Continuous phenomena such as polishing wear are represented within existing characteristics, plastic deformation requires adaptation of existing ones, and discrete patterns such as scratches necessitate the introduction of entirely new characteristics. A second strength is the sensitivity of the resulting tolerance regions, as small geometric variations can have a significant impact on functional behavior in high-performance systems such as bearing interfaces. The case study further indicates that the impact of individual characteristics cannot always be interpreted independently, as combinations such as scratch angle and depth may influence the system behavior in a coupled manner. Interaction effects therefore have to be considered when establishing embodiment-function relations. At the same time, the application reveals two challenges. The first concerns the effort of the method, which varies considerably across steps and depends strongly on the availability of technical documentation, manufacturing data, and suitable measurement and testing environments. The second challenge concerns the definition of appropriate descriptors for degradation features, which requires expert knowledge and may influence the resulting embodiment-function relations. For example, it remains unclear whether a scratch should be described by parameters such as angle, length, width, and depth, or by aggregated measures such as area or volume. The difficulty intensifies where multiple degradation patterns overlap within the same region, so that a clear and unambiguous description could not always be established. This is consistent with findings in the literature that subtractive reprocessing is often required to restore a well-defined embodiment state before further evaluation [56].

5.2. Positioning and limitations

Compared against the approaches listed in Table 1, the specific contribution of the UED lies in the elements it adopts from each of them and in what it adds. The unified characteristic space in the first layer builds on the formulation of embodiment in engineering design and manufacturing, where GPS [16] and its extensions such as GeoSpelling [18] define characteristics for nominal geometry and manufacturing-induced variations. The UED adopts this formulation but extends it toward degradation, where the set of relevant characteristics is not known in advance and therefore cannot be fixed at design time. For the detection and quantification of degradation, the UED draws on vision-based condition monitoring [27], but expresses the resulting observations as embodiment characteristics within the same formulation instead of introducing them as ad-hoc descriptors for isolated local defects. The introduction of artificial damage is likewise employed not as an end in itself but as a means to realize defined embodiment states for testing, whose results are embedded into the unified characteristic space rather than remaining single-mechanism observations. The characteristic space thereby becomes adaptive rather than fixed. In parameter-based models, the factor space is defined over the design variables of the nominal component, so that integrating degradation would require each pattern and feature to be introduced as an additional dimension. By structuring the characteristics into three categories and their interrelations, the UED supports these otherwise implicit decisions and makes degradation-induced dimensions accessible to such evaluations.

The second layer, the functionally derived tolerance regions, draws on conceptual frameworks such as the function-behavior-state modeler, which establishes the relation between embodiment and functional behavior on the level of attributes and states [34]. The UED adopts this perspective but quantifies the relation for the measured embodiment of an individual component. Condition monitoring likewise assesses individual components, yet infers their state from measured signals [47], whereas the UED derives functional behavior from the described embodiment and thereby indicates which characteristics have to be addressed by a reprocessing operation. A tolerance region corresponds to a solution space [42], as it delimits the region of characteristic values for which the required functional behavior is achieved. The assignment of R-strategies follows a margin-based logic [44], as it is determined by the distance between the embodiment state of an individual component and the boundary of this region. The UED thereby transfers the notions of admissible spaces and margins from the prospective design of a component type to the state-dependent evaluation of an individual, already degraded component. Beyond the two layers, the UED specifies which characteristics are functionally relevant and how they relate to functional behavior, which integrating architectures such as the digital twin leave open [50]. It therefore complements them rather than competing with them, while the acquisition, storage, and integration of the required data across the lifecycle remain a task for the surrounding information architecture.

Overall, the UED can be interpreted as a bridging approach that connects design-oriented, manufacturing-oriented, and degradation-oriented embodiment descriptions. While the approach is designed to be generalizable, its applicability to other components and systems with different functional mechanisms requires further validation, as the case study is limited to the specific component of an angle grinder spindle shaft and its functional principle. The case study also focuses deliberately on geometric characteristics, although material properties such as hardness or residual stresses can be incorporated through the same structuring principle. In addition, since the UED method has so far only been applied by its developers, no insights into how it is understood by other design engineers or researchers could yet be derived. The identification and quantification of functionally relevant characteristics could be further supported by integrating established approaches such as the contact and channel approach [9] or DoE screening [37]. The quantification of embodiment-function relations is furthermore based on a limited parameter space and controlled experimental conditions, and real-world applications may involve more complex interactions and variability from which new challenges may emerge. Finally, the application of the UED in this work is restricted to manual evaluation of functional behavior and the derivation of corresponding tolerance regions. The linkage to automated design decision-making, which would be necessary for scalable use in operational circular factories, was not the focus of this case study and requires further investigation.

5.3. Implications for circular manufacturing systems

The UED has significant implications for how decisions are prepared and processes are designed in circular manufacturing systems. For diagnostics, it enables a more comprehensive and structured assessment of used components. Instead of relying on isolated measurements or defect detection [23,24], multiple characteristics and their interactions can be considered simultaneously, allowing a more accurate identification of degradation states and their potential impact on functional behavior.

For reprocessing, the UED enables a shift from constraint-driven restoration to function-oriented modification. Since the influence of individual characteristics on functional behavior is quantified, reprocessing strategies can be tailored to achieve specific functional targets. This includes not only restoring nominal conditions but also intentionally modifying nominal characteristics, for example by adjusting diameters or surface properties, to improve performance or adapt components to new product generations, thereby enabling "perpetual innovative products" [3].

For design, the results provide a basis for developing more robust and circularity-oriented products. By identifying which embodiment characteristics are functionally relevant and how they interact, design engineers can derive targeted measures to reduce sensitivity to degradation or to enable more effective reprocessing. Overall, the UED supports a transition toward systematic, function-oriented evaluation, which is essential for the implementation of circular manufacturing systems.

6. Conclusion and outlook

Decision-making in circular manufacturing systems requires a consistent description of embodiment states that goes beyond the nominal design characteristics of linear production. This paper introduced the UED as a two-layered, state-dependent representation of mechanical components, supported by the UED method that guides its systematic development. The UED integrates design, manufacturing, and degradation perspectives into a unified characteristic space that adapts and extends as new lifecycle effects emerge. It further links the resulting embodiment characteristics to the functional behavior of the surrounding subsystem through functionally derived tolerance regions.

The case study on an angle grinder spindle shaft demonstrated the construction of the UED in a representative circular manufacturing scenario. The degradation patterns polishing wear, plastic deformation, and scratches were quantified against a statistical manufacturing baseline and embedded into the unified characteristic space, where existing nominal characteristics either remained sufficient, required adaptation, or had to be complemented by new spatially localized descriptors. Degradation therefore acts as a structural driver of the characteristic space rather than as a mere deviation within a fixed parameter set. The subsequent quantification of embodiment-function relations on a dedicated test bench translated this description into functionally derived tolerance regions, which enable data-driven decisions on reuse, reprocessing, and recycling as well as design adaptations across product generations and manufacturers.

Future research should reduce the reliance on expert judgment in the definition of degradation descriptors, for example through structured screening approaches or data-driven descriptor selection, and address the treatment of interacting or spatially overlapping degradation mechanisms. A further direction is the linkage to automated decision-making, which requires the transfer of the UED from a conceptual construct into a formally specified and machine-interpretable representation. An integrated product ontology provides a foundation for this transfer, as it formalizes the cross-generational description of embodiment characteristics, degradation states, and technical requirements [57]. A further challenge arises from the distribution of the required data across manufacturers, operators, and reprocessing sites, which approaches such as federated learning address by training models across distributed sources without exchanging the underlying data [58]. Finally, the scalability of the UED to component classes and functional principles beyond rotational machine elements should be investigated, including its application by engineers outside the developing team.

Overall, the UED provides a foundation for moving from static to state-dependent embodiment representations. By enabling a consistent link between the physical state of components and the functional behavior of the corresponding subsystem, it is an enabling element for the operation of circular manufacturing systems, in which value retention and product innovation can be reconciled through informed, function-oriented decisions at the level of individual components.

CRediT authorship contribution statement

Jonas Hemmerich: Writing – review & editing, Writing – original draft, Visualization, Methodology, Investigation, Formal analysis, Conceptualization. **Dominik Koch:** Writing – original draft, Visualization, Investigation, Formal analysis. **Victor Mas:** Writing – original draft, Conceptualization. **Nehal Afifi:** Writing – original draft, Conceptualization. **Edwin Blum:** Investigation, Formal analysis. **Gisela Lanza:** Writing – review & editing, Supervision. **Sven Matthiesen:** Writing – review & editing, Supervision. **Patric Grauberger:** Writing – original draft, Supervision, Project administration, Funding acquisition, Conceptualization.

Declaration of generative AI and AI-assisted technologies in the manuscript preparation process

During the preparation of this work, the authors used ChatGPT (OpenAI) and Claude (Anthropic) in order to improve the structure, readability, and phrasing of the manuscript. After using these tools, the authors reviewed and edited the content as needed and take full responsibility for the content of the publication.

Declaration of competing interest

The authors declare that they have no known competing financial interests or personal relationships that could have appeared to influence the work reported in this paper.

Acknowledgments

Funded by the Deutsche Forschungsgemeinschaft (DFG, German Research Foundation) - SFB 1574 - 471687386.

References

[1] Parker D, Riley K, Robinson S, Symington H, Tewson J, Jansson K, Ramkumar S, Peck D. Remanufacturing market study. European Remanufacturing Network (ERN); 2015, URL https://cris.vtt.fi/en/publications/remanufacturing-market-study.

[2] Ellen MacArthur Foundation. Towards a circular economy: Business rationale for an accelerated transition. 2015, URL https://www.ellenmacarthurfoundation.org/towards-a-circular-economy-business-rationale-for-an-accelerated-transition.

[3] Lanza G, Deml B, Matthiesen S, Martin M, Brützel O, Hörsting R. The vision of the circular factory for the perpetual innovative product. AT - Automatisierungstechnik 2024;72(9):774–88. http://dx.doi.org/10.1515/auto-2024-0012.

[4] Grauberger P, Dörr M, Lanza G, Kaiser J-P, Albers A, Düser T, Tusch L, Seidler M, Dietrich S, Schulze V, Matthiesen S. Enabling the vision of a perpetual innovative product – predicting function fulfillment of new product generations in a circular factory. AT - Automatisierungstechnik 2024;72(9):815–28. http://dx.doi.org/10.1515/auto-2024-0010.

[5] Theilig K, Lourenço B, Reitberger R, Lang W. Life cycle assessment and multi-criteria decision-making for sustainable building parts: criteria, methods, and application. Int J Life Cycle Assess 2024;29(11):1965–91. http://dx.doi.org/10.1007/s11367-024-02331-9.

[6] Du Y, Cao H, Liu F, Li C, Chen X. An integrated method for evaluating the remanufacturability of used machine tool. J Clean Prod 2012;20(1):82–91. http://dx.doi.org/10.1016/j.jclepro.2011.08.016.

[7] Jiang Z, Zhang H, Sutherland JW. Development of multi-criteria decision making model for remanufacturing technology portfolio selection. J Clean Prod 2011;19(17):1939–45. http://dx.doi.org/10.1016/j.jclepro.2011.07.010.

[8] Soares MDS, Vrancken J. Model-Driven User Requirements Specification using SysML. J Softw 2008;3(6):57–68. http://dx.doi.org/10.4304/jsw.3.6.57-68.

[9] Grauberger P, Wessels H, Gladysz B, Bursac N, Matthiesen S, Albers A. The contact and channel approach – 20 years of application experience in product engineering. J Eng Des 2020;31(5):241–65. http://dx.doi.org/10.1080/09544828.2019.1699035.

[10] Pahl G, Beitz W, Feldhusen J, Grote K-H. Engineering design. London: Springer London; 2007, http://dx.doi.org/10.1007/978-1-84628-319-2.

[11] Weber C. Modelling Products and Product Development Based on Characteristics and Properties. In: Chakrabarti A, Blessing LTM, editors. An anthology of theories and models of design: philosophy, approaches and empirical explorations. London: Springer; 2014, p. 327–52. http://dx.doi.org/10.1007/978-1-4471-6338-1_16.

[12] Gero JS, Kannengiesser U. The situated function–behaviour–structure framework. Des Stud 2004;25(4):373–91. http://dx.doi.org/10.1016/j.destud.2003.10.010.

[13] Söderberg R, Wärmefjord K, Carlson JS, Lindkvist L. Toward a Digital Twin for real-time geometry assurance in individualized production. CIRP Ann 2017;66(1):137–40. http://dx.doi.org/10.1016/j.cirp.2017.04.038.

[14] Morse E, Dantan J-Y, Anwer N, Söderberg R, Moroni G, Qureshi A, Jiang X, Mathieu L. Tolerancing: Managing uncertainty from conceptual design to final product. CIRP Ann 2018;67(2):695–717. http://dx.doi.org/10.1016/j.cirp.2018.05.009.

[15] Dadfarnia M, Sharp ME, Herrmann JW. Comprehensive evaluations of condition monitoring-based technologies in industrial maintenance: A systematic review. J Manuf Syst 2025;82:449–77. http://dx.doi.org/10.1016/j.jmsy.2025.06.015.

[16] ISO1101:2017-09. Geometrical product specifications (GPS) — Geometrical tolerancing — Tolerances of form, orientation, location and run-out. International Organization for Standardization; 2017.

[17] De Feo JA. Juran's quality handbook: The complete guide to performance excellence. Seventh edition. New York: McGraw-Hill Education; 2016.

[18] Dantan J-Y, Ballu A, Mathieu L. Geometrical product specifications — model for product life cycle. Computer-Aided Des 2008;40(4):493–501. http://dx.doi.org/10.1016/j.cad.2008.01.004.

[19] Schleich B, Anwer N, Mathieu L, Wartzack S. Skin Model Shapes: A new paradigm shift for geometric variations modelling in mechanical engineering. Computer-Aided Des 2014;50:1–15. http://dx.doi.org/10.1016/j.cad.2014.01.001.

[20] Zhang M, Shi Z, Mathieu L, Nabil A, Yang J. Geometric Product Specification of Gears: The GeoSpelling Perspective. Procedia CIRP 2015;27:90–6. http://dx.doi.org/10.1016/j.procir.2015.04.049.

[21] Koch D, Kaiser J-P, Stamer F, Stark R, Lanza G. Enhancing Visual Inspection in Remanufacturing: A Reinforcement Learning Approach with Integrated Robot Simulation. Procedia CIRP 2025;134:939–44. http://dx.doi.org/10.1016/j.procir.2025.02.228.

[22] Ye XW, Dong CZ, Liu T. A Review of Machine Vision-Based Structural Health Monitoring: Methodologies and Applications. J Sensors 2016;2016(1):7103039. http://dx.doi.org/10.1155/2016/7103039.

[23] Tabernik D, Šela S, Skvarč J, Skočaj D. Segmentation-based deep-learning approach for surface-defect detection. J Intell Manuf 2020;31(3):759–76. http://dx.doi.org/10.1007/s10845-019-01476-x.

[24] Liu R, Zhong D, Lyu H, Han J. A Bevel Gear Quality Inspection System Based on Multi-Camera Vision Technology. Sensors 2016;16(9):1364. http://dx.doi.org/10.3390/s16091364.

[25] Kaiser J-P, Gäbele J, Koch D, Schmid J, Stamer F, Lanza G. Adaptive acquisition planning for visual inspection in remanufacturing using reinforcement learning. J Intell Manuf 2025;36(7):4867–93. http://dx.doi.org/10.1007/s10845-024-02478-0.

[26] Wu Y, Zhou C, Sterkens W, Goedemé T, Dewulf W, Peeters JR. SCES: Surface condition evaluation system for electrical and electronic equipment reuse grading by combining defect detection and segmentation—A case study of laptops. Resour Conserv Recycl 2026;225:108608. http://dx.doi.org/10.1016/j.resconrec.2025.108608.

[27] Van Maele D, Poletto JC, De Geest R, Liao W, Ferreira NF, Neis PD, Fauconnier D, De Baets P. A vision-assisted condition monitoring framework for wear monitoring of gearboxes. Forsch Im Ingenieurwesen 2025;89(1):70. http://dx.doi.org/10.1007/s10010-025-00833-y.

[28] Zou L, Zeng D, Dong Y, Li J, Chen X, Zhao H, Lu L. Experimental and numerical study on the fretting wear-fatigue interaction evolution in press-fitted axles. Int J Fatigue 2023;175:107793. http://dx.doi.org/10.1016/j.ijfatigue.2023.107793.
[29] ISO10303:2024-01. Industrial automation systems and integration – Product data representation and exchange. International Organization for Standardization; 2024.
[30] Ameri F, Dutta D. Product Lifecycle Management: Closing the Knowledge Loops. Computer-Aided Des Appl 2005;2(5):577–90. http://dx.doi.org/10.1080/16864360.2005.10738322.
[31] Kiritsis D. Closed-loop PLM for intelligent products in the era of the Internet of things. Computer-Aided Des 2011;43(5):479–501. http://dx.doi.org/10.1016/j.cad.2010.03.002.
[32] Sanderson D, Chaplin JC, Ratchev S. A Function-Behaviour-Structure design methodology for adaptive production systems. Int J Adv Manuf Technol 2019;105(9):3731–42. http://dx.doi.org/10.1007/s00170-019-03823-x.
[33] Wu B, Jiang Z, Zhu S, Zhang H, Wang Y. A customized design method for upgrade remanufacturing of used products driven by individual demands and failure characteristics. J Manuf Syst 2023;68:258–69. http://dx.doi.org/10.1016/j.jmsy.2023.04.004.
[34] Umeda Y, Ishii M, Yoshioka M, Shimomura Y, Tomiyama T. Supporting conceptual design based on the function-behavior-state modeler. Artif Intell Eng Des Anal Manuf 1996;10(4):275–88. http://dx.doi.org/10.1017/S0890060400001621.
[35] Umeda Y, Kondoh S, Shimomura Y, Tomiyama T. Development of design methodology for upgradable products based on function–behavior–state modeling. AI EDAM 2005;19(3):161–82. http://dx.doi.org/10.1017/S0890060405050122.
[36] Kang E, Jackson E, Schulte W. An approach for effective design space exploration. In: Calinescu R, Jackson E, editors. Foundations of computer software. Modeling, development, and verification of adaptive systems. Berlin, Heidelberg: Springer; 2011, p. 33–54. http://dx.doi.org/10.1007/978-3-642-21292-5_3.
[37] Montgomery DC. Design and analysis of experiments. 10th edition. Hoboken, NJ: Wiley; 2019.
[38] Tahera K, Wynn DC, Earl C, Eckert CM. Testing in the incremental design and development of complex products. Res Eng Des 2019;30(2):291–316. http://dx.doi.org/10.1007/s00163-018-0295-6.
[39] Liu J, Ni H, Zhou R, Li X, Xing Q, Pan G. A Simulation Analysis of Ball Bearing Lubrication Characteristics Considering the Cage Clearance. J Tribol 2023;145(4):044301. http://dx.doi.org/10.1115/1.4056358.
[40] Křupka I, Šperka P, Hartl M, Xue Jin S, Xiao Yang C. Effect of real longitudinal surface roughness on lubrication film formation within line elastohydrodynamic contact. Tribol Int 2010;43(12):2384–9. http://dx.doi.org/10.1016/j.triboint.2010.08.007.
[41] Zhang W, Wang Z, Li X, Xiang S. Physics-integrated intelligent method for propeller aerodynamic property predictions of electric aircraft. Eng Appl Artif Intell 2026;173:114408. http://dx.doi.org/10.1016/j.engappai.2026.114408.
[42] Zimmermann M, Von Hoessle JE. Computing solution spaces for robust design. Internat J Numer Methods Engrg 2013;94(3):290–307. http://dx.doi.org/10.1002/nme.4450.
[43] Thunnissen DP, Tsuyuki GT. Margin Determination in the Design and Development of a Thermal Control System. In: International conference on environmental systems. Colorado Springs, Colorado, United States; 2004, p. 2004–01–2416. http://dx.doi.org/10.4271/2004-01-2416.
[44] Brahma A, Wynn DC. Margin value method for engineering design improvement. Res Eng Des 2020;31(3):353–81. http://dx.doi.org/10.1007/s00163-020-00335-8.
[45] Park G-J, Lee T-H, Lee KH, Hwang K-H. Robust Design: An Overview. AIAA J 2006;44(1):181–91. http://dx.doi.org/10.2514/1.13639.
[46] Feng K, Ji JC, Ni Q, Beer M. A review of vibration-based gear wear monitoring and prediction techniques. Mech Syst Signal Process 2023;182:109605. http://dx.doi.org/10.1016/j.ymssp.2022.109605.
[47] Li Y, Wang S, Deng Z. Intelligent fault identification of rotary machinery using refined composite multi-scale Lempel–Ziv complexity. J Manuf Syst 2021;61:725–35. http://dx.doi.org/10.1016/j.jmsy.2020.05.004.
[48] Häderle P, Merkle L, Dazer M. Vibration analysis for early pitting detection during operation. Forsch Im Ingenieurwesen 2024;88(1):15. http://dx.doi.org/10.1007/s10010-024-00743-5.
[49] Grieves M, Vickers J. Digital Twin: Mitigating Unpredictable, Undesirable Emergent Behavior in Complex Systems. In: Kahlen F-J, Flumerfelt S, Alves A, editors. Transdisciplinary perspectives on complex systems. Cham: Springer International Publishing; 2017, p. 85–113. http://dx.doi.org/10.1007/978-3-319-38756-7_4.
[50] Kerin M, Pham DT, Huang J, Hadall J. A generic asset model for implementing product digital twins in smart remanufacturing. Int J Adv Manuf Technol 2023;124(9):3021–38. http://dx.doi.org/10.1007/s00170-022-09295-w.
[51] Gericke K, Eckert C, Stacey M. What do we need to say about a design method? In: DS 87-7 Proceedings of the 21st international conference on engineering design (ICED 17). Design theory and research methodology, vol. 7, Vancouver, Canada; 2017, p. 101–10, URL https://www.designsociety.org/publication/39810/what_do_we_need_to_say_about_a_design_method.
[52] Hemmerich J, Kirn A, Walter G, Wittig C, Grauberger P, Matthiesen S. How to deal with products in circular economy: an approach to model specific design knowledge illustrated at the example of a circular factory for angle grinders. Proc Des Soc 2025;5:1983–92. http://dx.doi.org/10.1017/pds.2025.10212.
[53] ISO3245:2023-01. Rolling bearings. Needle roller bearings with drawn cup and without inner ring. Boundary dimensions, geometrical product specifications (GPS) and tolerance values. International Organization for Standardization; 2023.
[54] ISO15243:2017-03. Rolling bearings - Damage and failures - Terms, characteristics and causes. International Organization for Standardization; 2017.
[55] Mas V, Hemmerich J, Klesen A, Münch M, Afifi N, Grauberger P, Matthiesen S. Testing Environments for Data Driven Prediction of Functional Behavior and Reliability in the Circular Factory. In: Proceedings of the conference on circular production systems and technologies, vol. 1, Heidelberg: SpringerNature; 2026, (accepted for publication).
[56] Barragan De Los Rios GA, Ferreira R, Mariani FE, da Silva EJ, Coelho RT. Study of the surface roughness of a remanufactured bimetallic AISI 1045 and 316L SS part obtained by hybrid manufacturing (DED/HSM). Int J Adv Manuf Technol 2023;124(9):3185–99. http://dx.doi.org/10.1007/s00170-022-09179-z.
[57] Vlajic K, Moser G, Hemmerich J, Mas V, Afifi N, Hoffmann E, Thapa R, Grauberger P, Matthiesen S, Albers A, Düser T. An integrated Ontology for the Perpetual Innovative Product in the Circular Factory. In: Proceedings of the 1st conference on circular production systems and technologies. Berlin: Springer Nature Conference Proceedings; 2026, (accepted for publication).
[58] Li X, Fan W, Yang S, Zhang W, Li X. Flexible Federated Learning in Machinery Fault Diagnostics with Light Communication. IEEE/CAA J Autom Sin 2026;13(3):680–91. http://dx.doi.org/10.1109/JAS.2025.125414.